

GROUNDWATER CHEMISTRY IN THE COLUMBIA RIVER BASALT GROUP, COLUMBIA BASIN, WASHINGTON

by Ellen E. Svadlenak & Lee J. Florea

WASHINGTON
GEOLOGICAL SURVEY
Report of Investigations 48
July 2025

INTERNALLY AND EXTERNALLY REVIEWED



WASHINGTON STATE DEPARTMENT OF
NATURAL RESOURCES
WASHINGTON GEOLOGICAL SURVEY

GROUNDWATER CHEMISTRY IN THE COLUMBIA RIVER BASALT GROUP, COLUMBIA BASIN, WASHINGTON

by Ellen E. Svadlenak & Lee J. Florea

WASHINGTON
GEOLOGICAL SURVEY
Report of Investigations 48
July 2025

*This publication was reviewed by four external experts.
This publication was also reviewed by Survey
geologists, editors, and cartographers.*



WASHINGTON STATE DEPARTMENT OF
NATURAL RESOURCES
WASHINGTON GEOLOGICAL SURVEY

DISCLAIMER

Disclaimer of Warranties. No express or implied warranty of any kind is made regarding the information contained herein, including, but not limited to, the warranty of merchantability, warranty of fitness for a particular purpose, or warranties of content, completeness, accuracy, reliability, usefulness, or that use would not infringe on privately-owned rights.

Use at Your Own Risk. The information presented here is intended for use as a general screening tool in community planning or for creating awareness and understanding of geologic information and is neither intended to constitute advice nor is it to be used as a substitute for site-specific advice from a licensed professional. You use this information at your own risk and should not act (or refrain from acting) based upon the information without independently verifying the information and, as appropriate, obtaining professional advice regarding your particular facts and circumstances.

Limitation on Liability. User agrees there shall not be liability on the State of Washington, Washington Department of Natural Resources, or their officers, agents, representatives, or employees for any damages allegedly resulting from any use of or reliance on this information. Under this limitation, there shall be no liability for any damages whatsoever, including but not limited to any damages in contract or tort for compensatory, consequential, punitive, direct, indirect, or special damages such as personal injuries, property damage, loss of profits, or any other losses or expenses.

No Endorsement. Reference herein to any specific commercial product, process, or service by trade name, trademark, manufacturer, or otherwise, does not constitute or imply its endorsement, recommendation, or favoring. Further, the views and opinions of authors expressed herein do not necessarily state or reflect those of the State of Washington or any agency thereof.

WASHINGTON STATE DEPARTMENT OF NATURAL RESOURCES

Dave Upthegrove—*Commissioner of Public Lands*

WASHINGTON GEOLOGICAL SURVEY

Casey R. Hanell—*State Geologist*

Jessica L. Czajkowski—*Assistant State Geologist*

Ana Shafer—*Assistant State Geologist*

Alexander N. Steely—*Assistant State Geologist*

Washington State Department of Natural Resources Washington Geological Survey

Mailing Address:

MS 47007

Olympia, WA 98504-7007

Street Address:

Natural Resources Bldg, Rm 148

1111 Washington St SE

Olympia, WA 98501

Phone: 360-902-1450

Fax: 360-902-1785

Email: geology@dnr.wa.gov

Website: <http://www.dnr.wa.gov/geology>



Publications and Maps:

[www.dnr.wa.gov/programs-and-services/geology/
publications-and-data/publications-and-maps](http://www.dnr.wa.gov/programs-and-services/geology/publications-and-data/publications-and-maps)

Washington Geology Library Searchable Catalog:

[www.dnr.wa.gov/programs-and-services/geology/
washington-geology-library](http://www.dnr.wa.gov/programs-and-services/geology/washington-geology-library)

Suggested Citation: Svadlenak, E. E.; Florea, L. J., 2025, Groundwater chemistry in the Columbia River Basalt Group, Columbia Basin, Washington: Washington Geological Survey Report of Investigations 48, 21 p. text and 1 Microsoft Excel file.
[https://dnr.wa.gov/sites/default/files/2025-07/ger_ri48_groundwater_columbia_basin.zip]

Contents

Introduction	2
Architecture of the CRBG aquifer system	2
Water-rock reactions in the CRBG	3
Methods.....	4
Data compilation.....	4
Water sampling	5
Data analysis	5
Results	6
Analytical groundwater chemistry	6
Field measurements and bulk chemistry.....	6
Cations and anions	6
Stable and radioactive isotopes.....	6
Spatial variation in groundwater chemistry	9
Selected comparisons with formation and depth	9
Selected comparisons between analytes	10
Modeled groundwater chemistry	11
Clusters of groundwater chemistry	12
Discussion	13
Primary controls on CRBG groundwater chemistry	14
Vertical stratification of CRBG groundwater.....	14
Spatial distribution of CRBG groundwater types	16
CRBG groundwater groups	16
Isotopic profile of CRBG groundwater.....	17
Conclusions	17
Acknowledgments.....	18
References	18

FIGURES

Figure 1. Generalized extent and stratigraphy of the Columbia River Basalt Group formations considered in this study	2
Figure 2. Schematic of the flow structures found in a typical Columbia River Basalt flow.	3
Figure 3. Primary mineralogy of the Grande Ronde Basalt of the Columbia River Basalt Group with associated hydrothermal alteration products	4
Figure 4. Map depicting the distribution of samples in the groundwater chemistry database	5
Figure 5. Piper and Durov diagrams showing the proportional abundance of principal cations and anions in groundwaters from the Columbia River Basalt Group.....	8
Figure 6. Chadha Plot of groundwater samples from the Columbia River Basalt Group	8
Figure 7. Scatterplot showing the $\delta^{18}\text{O}$ and $\delta^2\text{H}$ of groundwaters in the Columbia River Basalt Group	8
Figure 8. Scatterplot showing the variation of cation ratio $([\text{Na}] + [\text{K}]) / ([\text{Na}] + [\text{K}] + [\text{Ca}] + [\text{Mg}])$ as a function of ^{14}C (in % modern) in groundwaters from the Columbia River Basalt Group.....	9
Figure 9. Scatterplot comparing temperature with depth in Columbia River Basalt Group groundwater	9
Figure 10. Scatterplot comparing the concentration of total dissolved solids (TDS) with depth in Columbia River Basalt Group groundwater.....	10
Figure 11. Scatterplot comparing calcite saturation index (SI) with depth in Columbia River Basalt Group groundwater.....	11

Figure 12. Diagram depicting mineral stability fields relative to calculated ion concentrations and activity ratios in Columbia River Basalt Group groundwater.....	11
Figure 13. Scatterplot comparing the saturation index (SI) with depth for mordenite (a zeolite), amorphous silica, and basaltic glass	12
Figure 14. Plots from principal component analyses (PCA) that show the eigenvalue weighting of each variable for PC1, PC2, and PC3	12
Figure 15. Scatterplots of Columbia River Basalt Group groundwaters on the results of the principal component analysis.....	13
Figure 16. Scatterplot comparing the cation ratio $([Na] + [K]) / ([Na] + [K] + [Ca] + [Mg])$ as a function of depth in groundwaters from the Columbia River Basalt Group.....	15
Figure 17. Map depicting sample sites classified by group from the hierarchical cluster analysis.....	16

TABLES

Table 1. Data types and analytes in groundwater chemistry dataset for the Columbia basin...	5
Table 2. Summary statistics for select analytes	7
Table 3. The proportion of variance explained by each principal component.....	12

Groundwater Chemistry in the Columbia River Basalt Group, Columbia Basin, Washington

by Ellen E. Svadlenak¹ & Lee J. Florea¹

¹ Washington Geological Survey
MS 47007
Olympia, WA 98504-7007

INSIGHTS

- To aid in future groundwater management and clean energy projects, we created a new groundwater chemistry database for the Columbia basin that includes 1,537 water samples from wells in the basin.
- The Columbia River Basalt Group (CRBG) aquifer system includes upper (<650 m deep) and lower (>750 m deep) divisions in this dataset marked by a distinct change in groundwater temperature, chemistry, and isotopic profile.
- The upper CRBG aquifer division is enriched in alkaline-earth metals from oxidative and carbonation weathering. These metals precipitate as carbonate in the anoxic lower CRBG aquifer division, where alkali metals from cation exchange reactions dominate the chemistry.
- Despite increasing total dissolved solids with depth, only three of the deepest samples are saline, which suggests that the groundwaters of the CRBG aquifer system remain potable down to a depth of >750 m, though more sampling is needed to confirm this.

EXECUTIVE SUMMARY

The Columbia River Basalt Group (CRBG) is an important source of potable and irrigation water in the Columbia basin of central and eastern Washington. The thickness and basaltic composition of the CRBG are of growing interest for geologic carbon sequestration, geothermal resources, thermal energy storage, and hydrogen storage. This study of 1,537 groundwater samples from 1,282 sample locations in the CRBG builds upon a century of water quality studies and expands prior work to new sampling, wells at the basin margin, oil and gas wells, and thermal and mineral springs. This report differs from much of the previous work in that it characterizes groundwater across the extent of the CRBG in Washington east of the Columbia River Gorge and focuses on deeper groundwater, where data are sparse, to distinguish deeper CRBG groundwaters from those at shallower depths. The intent of the work is to help inform decision-making around which parts of the CRBG aquifer may be suitable for geothermal and carbon sequestration applications.

The dataset that accompanies this report contains geochemical results for 74 analytes, of which 26 were used for further analysis. Results of chemical summary diagrams, bivariate regressions, modeled mineral solubility, principal component analyses, and a hierarchical cluster analysis for these 26 analytes support the range of observations noted by prior work and provide additional insight into water-rock reactions in the CRBG aquifer. In addition to variations with depth in dissolved ions, stable isotopes, and radiometric carbon, this study also identifies patterns between these analytes and the geologic setting, including the nature of geologic structures, interflow composition, and sub-basalt lithology. This work finds that there is a distinction between an upper CRBG aquifer system with active groundwater circulation in the Holocene and characterized by Ca-Mg-HCO₃-type groundwater and a lower CRBG aquifer system that is modestly thermal, relatively stagnant, and comprised of Na-Cl-type groundwaters of Pleistocene age and older. These groundwater data suggest active circulation of groundwater between the surface and a depth of 650 to 750 m, at which depth higher permeability in the lower Wanapum Basalts and in the underlying Vantage sedimentary interbeds encourage horizontal groundwater flow. At depths >750 m in these data, lower permeability in the upper Grand Ronde Basalt inhibits vertical mixing of water, trapping stagnant lower CRBG groundwater below this horizon and isolating the deeper, older waters from the upper CRBG aquifer waters. The depth to this transition is uncertain given a limited dataset at depth and may vary due to structural and other emplacement controls on the basalt.

Perhaps the most telling result of this investigation is that only three of the samples in the dataset are saline, using total dissolved solids >10,000 mg/L as the definition. The highest concentrations of total dissolved solids are less than 1,700 mg/L except for three deep oil and gas wells, even at depths >1,300 m. While it is possible, and even quite likely, that CRBG groundwaters at depths >3,000 m are saline, the lack of samples at these depths limits interpretations about deeper groundwater at depths >750 m.

The freshwater nature of most CRBG groundwater, even that which may be coeval with the emplacement of basalt, is notable and speaks to the non-marine origins of the connate water in the Columbia basin and the slow pace of water-rock interactions in these deeper settings. Carbon sequestration and other subsurface activities which require saline environments in the present regulatory framework are unlikely to be feasible shallower than 1,300 m to ensure protection of freshwater sources. Future studies would be needed to characterize deeper CRBG groundwater to explore for the saline waters needed for thermal energy storage and carbon sequestration.

INTRODUCTION

The Columbia River Basalt Group (CRBG) is an important source of potable and irrigation water in the Columbia basin of central and eastern Washington (Bauer and Hansen, 2000). CRBG units are potential targets for potable water storage (Burt and others, 2009; Nelson and Melady, 2014), thermal energy storage (Svadlenak, 2019; Burns and others, 2020), and geologic carbon sequestration (Zakharova and others, 2012; Cao and others, 2024). Understanding the chemistry of CRBG groundwater is particularly important as reactions between native waters, injected fluids, and the aquifer matrix can have significant impacts on chemistry, aquifer porosity and permeability, and thus on the efficacy of aquifer or thermal energy storage projects.

This report summarizes the geochemical patterns and trends observed in a companion dataset of 1,537 individual groundwater chemistry samples from the CRBG aquifer system, of which 1,519 samples were compiled from previous work and 18 samples represent new analyses. This report also interprets the water-rock interactions guiding groundwater chemistry in the CRBG, extending and refining prior interpretations from a body of literature that spans more

than a century. This dataset will be useful for those developing new groundwater supply points in the basin and those looking into the feasibility of aquifer storage and recovery, carbon sequestration, and thermal energy storage.

Architecture of the CRBG aquifer system

The CRBG aquifer system is a subset of the Columbia Plateau regional aquifer system (Kahle and others, 2011), which includes the CRBG aquifer system and alluvial and colluvial valley-fill aquifers. The CRBG dates to between 17.5 and 6 Ma (Tolan and others, 2009a) and comprises more than 300 individual basalt flows, with the Grande Ronde Basalt (16 to 15.6 Ma) constituting the most voluminous sequence (Barry and others, 2010). Overlying the Grande Ronde are the Wanapum and Saddle Mountains basalts (Fig. 1). Collectively, the CRBG extends over 210,000 km² and originated from fissure dikes in western Idaho, eastern Washington, and northern Oregon (Fig. 1). Erupting lavas inundated the Columbia basin and flowed through the Columbia trans-arc lowland to flood the Willamette Valley in Oregon, before reaching the Pacific Ocean (Reidel and others, 2013). The CRBG is more than 3,000 m thick in the core of the Columbia basin (Tolan and others, 2009b). Basalt stratigraphy in the CRBG is differentiated by paleomagnetism, radiometric dating, and whole-rock chemistry (Tolan and others, 2009a).

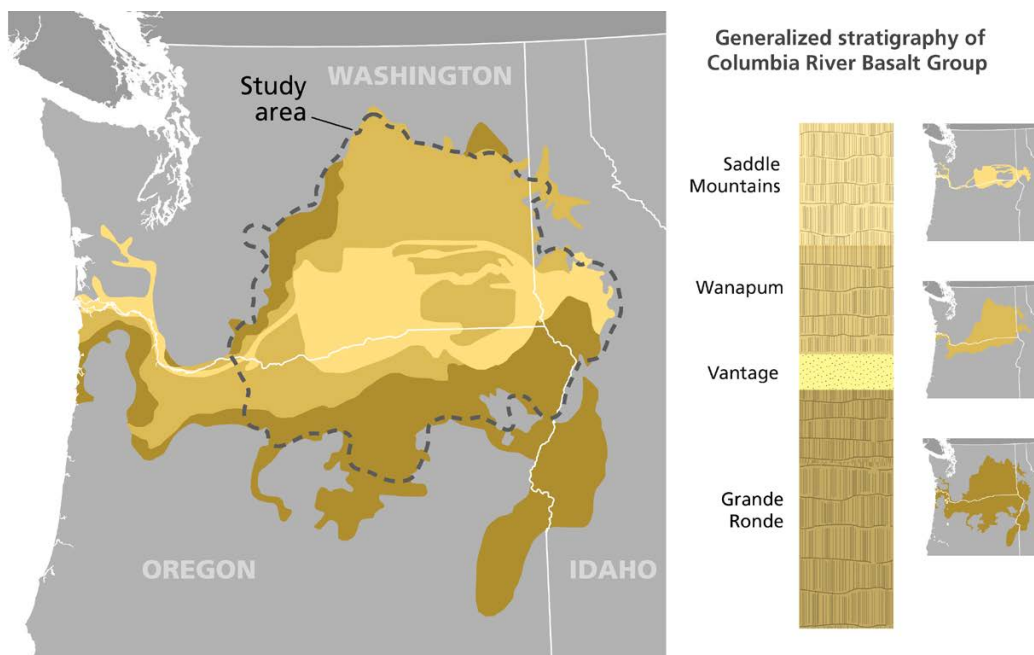


Figure 1. Generalized extent and stratigraphy of the Columbia River Basalt Group formations considered in this study. Each formation is comprised of a series of individual basalt flows, while the Vantage Member is a sedimentary interbed.

CRBG basalt flows have flow interiors and exteriors with highly contrasting permeability (Fig. 2; Reidel and others, 2013). The flow interiors have dense, massive colonnades and entablature that are five orders of magnitude less permeable than flow tops and bottoms (Tolan and others, 2009c), so the flow exteriors are the water-bearing zones of the CRBG. Basalt flow tops are commonly vesicular and (or) scoriaceous due to rapid cooling and degassing and may have a thick breccia or paleosol. Individual basalt flows may be separated by fluvial or lacustrine sediments deposited during the time between basalt flows. In some areas, these interflow units are water-bearing horizons in the aquifer system (Lindsey and others, 2009). In other areas, these same interflow units are clay rich and of low permeability, acting as aquitards. Where basalt flows invaded water bodies, basalt flow bottoms and margins frequently developed pillow structures in a palagonite matrix of altered volcanic glass, or hyaloclastite (Hooper, 1982).

The stratiform nature of the basalt flows creates a stacked series of semi-confined to confined groundwater flow units, together comprising a CRBG aquifer system that is highly anisotropic. Groundwater flow along the basalt flow margins and interflow units is from areas of recharge in uplands to areas of discharge along deeply incised rivers (Tolan and others, 2009a; Kahle and others, 2011). In contrast, vertical groundwater flow in the aquifer system is limited to zones where basalt flows are truncated by an erosional window or flow pinch out, where faults or fractures have enhanced vertical permeability, or where CRBG flow units are cross connected by wells (Tolan and others, 2009c). Regional groundwater flow is to the southwest, along the average dip of the basalts (Lindsey and others, 2009).

Characteristic intraflow structures and stratigraphy in Columbia River Basalt Group lava flows.

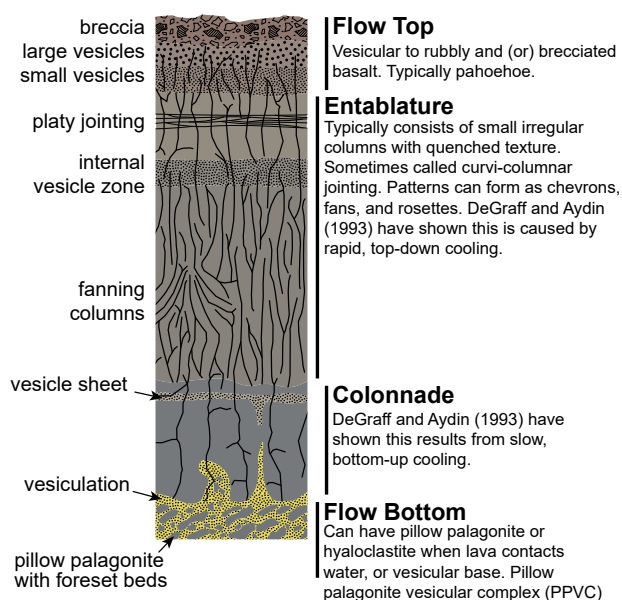


Figure 2. Schematic of the flow structures found in a typical Columbia River Basalt flow. The interflow zones are sedimentary units located below the flow bottoms and above the flow tops. (modified from Reidel and others, 2013).

Antecedent landforms, geologic structures, and eruption vents compartmentalize groundwater flow in the CRBG aquifer system. While many basalt flow units are planar, they thicken and thin according to the paleotopography. Where basalt flows followed the ancestral valleys of the Columbia and Snake Rivers, they were channelized and taper or pinch laterally (Fig. 1; Long and Wood, 1986). In the Yakima Fold and Thrust Belt, some flows thinned or overlapped contemporaneous deformation and uplift (Reidel and others, 2003) and other flows developed extension fractures along anticlinal axes (Hooper and Conrey, 1989). These faults and folds created groundwater sub-basins (Lite, 2013). In the Palouse slope of eastern Washington, the Chief Joseph dike swarm compartmentalizes groundwater between impermeable vertical dikes of basalt (Reidel and others, 2016).

The vertical permeability along faults and fractures is strongly dependent on confinement pressure, presence and composition of fault gouge, and whether secondary mineralization has occurred. At shallow depths, stress release from reduced overburden can cause fracture apertures to widen (Ferguson, 1967), including the columnar joints in flow interiors and stress fractures from brittle deformation. This allows for infiltration of meteoric recharge. At depth, joint and fracture apertures remain closed or may be annealed by secondary mineralization and mineral alteration products. Brecciated fault gouge can be quite permeable; however, the growth of clays and other secondary minerals from weathering reactions can reduce permeability along faults, limiting both vertical and horizontal movement of water (Burt and others, 2009; Tolan and others, 2009c).

Water-rock reactions in the CRBG

Examinations of groundwater chemistry in the CRBG aquifer system have largely focused on groundwater recharge (Medici and Langman, 2022) and residence time (Duckett and others, 2020; Johnson and others, 2024). Many of those studies consider groundwater chemistry through the lens of water quality and its relationship to land use and end utilization (Tolan and others, 2009c). In this study, we peer deeper into the geochemistry of CRBG groundwater, both physically and figuratively, to provide a framework for understanding the source of spatial patterns in groundwater chemistry in the Columbia basin. We build upon existing literature that associates CRBG groundwater chemistry to the residence time along regional flow paths (Hansen and others, 1994), the water-rock interactions along that flow path, and the reaction rates guided by the mineralogy and porosity of the aquifer matrix (Hearn and others, 1990).

The basalt of the CRBG is tholeiitic and includes plagioclase feldspar, pyroxene (augite), and iron oxides (mostly titanomagnetite). It also includes minor amounts of apatite, olivine, and sulfides (Hooper, 1982; Soderberg and Wolff, 2023). The interflow sedimentary units have varying mineralogy depending on the source provenance.

Chemical weathering in the CRBG is controlled by availability of reactants, areas of mineral surfaces exposed to groundwater, and rates of groundwater flow. One pathway for this weathering is oxidation from meteoric recharge. A second pathway is reactivity with carbon dioxide dissolved in groundwater. A third pathway is through cation exchange between a mineral and surrounding

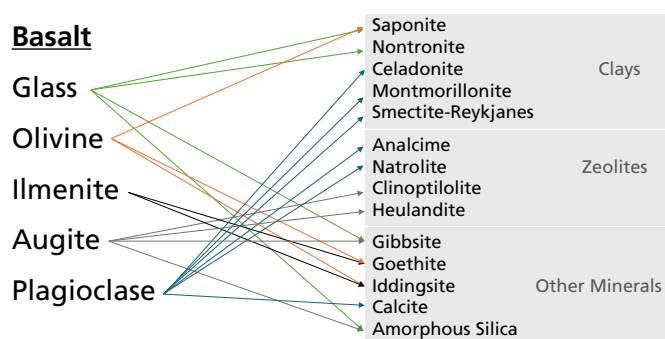


Figure 3. Primary mineralogy of the Grande Ronde Basalt of the Columbia River Basalt Group on the left with the associated hydrothermal alteration products on the right (modeled after Deutsch and others, 1982; Hearn and others, 1989; Tolan and others, 2009c).

groundwater. Groundwater composition can change, and therefore chemical weathering rates, based on injection activities (e.g., increased oxygen in the case of aquifer storage and recovery (ASR)). In these reaction pathways, the size of the reaction surface is a first order control on the rate of weathering—greater surface areas in vesicles, breccias, palagonite, and interflow sediments are more reactive.

The rate of groundwater circulation is a second order control—where groundwater is stagnant, reaction rates diminish as groundwaters reach saturation with respect to minerals. For example, Deutsch and others (1982) found that groundwater sampled from the CRBG at and surrounding the Hanford Site, Washington, a decommissioned nuclear production site, was in equilibrium with calcite, amorphous silica, and the zeolite wairakite. They also found that the groundwater was saturated to oversaturated with respect to secondary clay minerals and ferric hydroxide ($\text{Fe}(\text{OH})_3$).

Chemical weathering of CRBG and interflow minerals leads to dissolved solids in solution and alteration products at the site of weathering. These dissolved solids can result in secondary mineralization elsewhere in the CRBG aquifer system. Primary alteration products and secondary minerals are summarized in Figure 3 and include amorphous silica, cryptocrystalline quartz, smectites and other clays, zeolites, and iron oxides (Deutsch and others, 1982; Hearn and others, 1989; Tolan and others, 2009c). Nontronite (an iron-rich smectite) and goethite (an iron oxide) are among the most prevalent alteration products that form in the early stages of basalt weathering (Benson and Teague, 1982) at depths <1,000 ft (Hearn and others, 1990) with montmorillonite and kaolinite precipitating at later stages of feldspar, apatite, and titanomagnetite decomposition (Baker and others, 2016). As weathering progresses, clinoptilolite or other zeolites are formed along with silica and clays (Benson and Teague, 1982). Celadonite (a mica group mineral) has been found in basalt flow tops of the Grande Ronde Formation, filling vesicles and replacing the groundmass (Cummings and others, 1989; Baker and Niell, 2017). The potassium for celadonite formation comes from the dissolution of basaltic glass while the magnesium and iron are weathering byproducts of groundmass augite (Baker and others, 2012).

Chemical weathering reactions in the CRBG are temperature dependent—as temperatures increase, silicate solubility

increases while carbonate solubility decreases. Studies by Hearn and others (1990) and Benson and Teague (1982) found that almost all alteration occurs below 100 °C, and that trace amounts of calcite are ubiquitous throughout the CRBG. However, Burns and others (2015) identified a decrease in permeability below 600 m depth and hypothesized it was the result of increased carbonate precipitation related to increased heat flow at depth. This decrease in permeability may also be a product of meteoric weathering during subaerial exposure between the emplacement of the Grand Ronde Formation and later basalt flows.

METHODS

Groundwater chemistry data were aggregated from existing sources and collected for new samples acquired in 2023–2024. These data are provided in a spreadsheet that accompanies this report. The data are also viewable on the Washington Geological Survey (WGS) Geologic Information Portal (geologyportal.dnr.wa.gov) and downloadable in file geodatabase format from the WGS website (dnr.wa.gov/programs-and-services/geology/publications-and-data/gis-data-and-databases). Note that the Portal and file geodatabase formats will be updated as new data become available and may not match exactly the data analyzed in this report. Analyses of these data in the accompanying spreadsheet include regressions on scatterplots, reaction models in geochemical software, and population models in statistical software packages.

Data compilation

Existing groundwater chemistry data in this project are compiled from hydrogeologic reports by Washington State agencies and federal agencies, Washington State and federal data repositories, peer-reviewed literature, student theses and dissertations, and consultants' reports. Additional new data were collected by WGS staff. The sampled groundwaters include springs, water wells, oil and gas wells, and a carbon sequestration test well. The dataset is limited to the CRBG aquifer system and does not draw data from affiliated surficial and alluvial aquifers. The dataset also excludes sites that are explicitly sampled or monitored for anthropogenic contamination. Many sites were sampled more than once during the 125-year span of the dataset. The distribution of the data is concentrated in areas of the central basin and the Hanford Site that have received significant previous study.

The compiled dataset links geochemical analysis results with sample depth and CRBG unit (Fig. 4). Some samples have an association with a specific CRBG formation. Other samples aggregate water from more than one CRBG formation. In some cases, samples that list a CRBG unit at the sampling depth do not include the top and base of the sample intervals and thus may represent open borehole conditions and potential hydrologic mixing. A smaller subset, comprising the data from oil and gas wells and from springs, have no listed CRBG association. Sample data (Table 1) include site information; measured field parameters and bulk chemistry data; analytical measurements of major cations and anions, including the speciation of carbon, nitrogen, and sulfur; contributions of carbon, nitrogen, and phosphorous from organic sources; metals and trace elements; and the stable isotopes, radioactive isotopes, and the radiological

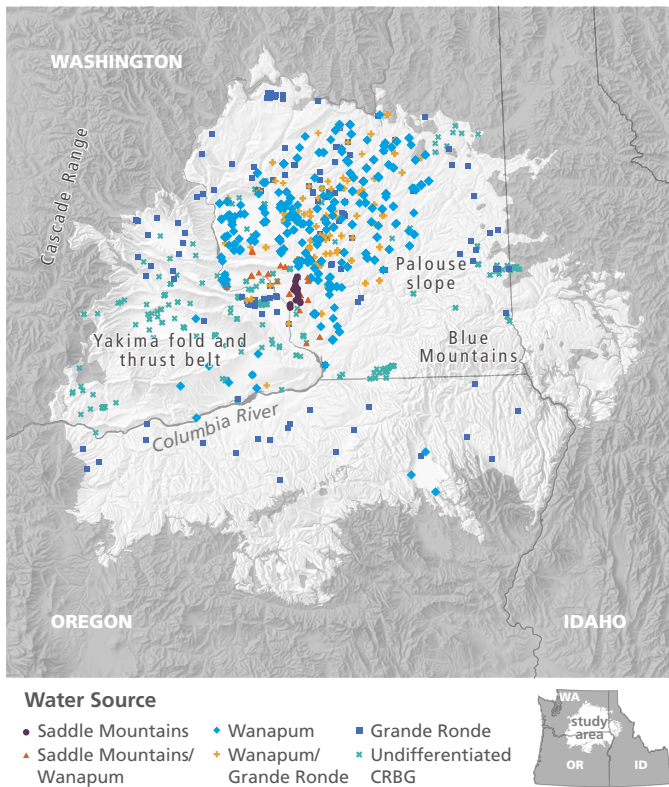


Figure 4. Map depicting the geographic boundary of a portion of the Columbia River Basalt Group in the Columbia Basin. The distribution of samples in the companion groundwater chemistry database are shown with sites classified by the listed formation at the sampling depth.

measurements of alpha and beta particles. Most samples only have results for a portion of the analytes in the dataset.

Water sampling

WGS sampled 15 wells during summer 2023 and one artesian well and two springs during spring 2024. Analytical results for these samples are included in the accompanying spreadsheet. Data collected in the field at the time of sampling include measurements of temperature (T), pH, specific conductance (SpC), dissolved oxygen (DO), and oxidation-reduction potential (ORP) collected using a YSI Pro-DSS hand-held sonde calibrated prior to each visit using pH 4, 7, and 10 standards, a 1,000 μ S solution for SpC, and Zobell solution. Onsite data were acquired to determine alkalinity and speciate carbonate with the inflection-point method using a HACH digital titrator and Oakton pH meter. Water samples for ion analysis were filtered using positive pressure through 0.45 micron cellulose nitrate filters and collected in high-density polyethylene (HDPE) bottles kept at 4°C until time of analysis at an accredited laboratory using standard methods for ion chromatography, atomic absorption, and turbidimetric light absorption. Samples for cations were preserved using 2 ml of 6N nitric acid (HNO_3) per 250 mL of sample. Samples for stable isotopes were collected in borosilicate vials and processed on a Picarro cavity ring-down spectrometer at Indiana University-Indianapolis for $\delta^2\text{H}$ and $\delta^{18}\text{O}$ and using an ion-ratio mass spectrometer at the University of Illinois for $\delta^{13}\text{C}$. Reporting methods for stable isotopes include standardization

Table 1. Data types and analytes in groundwater chemistry dataset for the Columbia basin.

Data types	Analytes
Site Information	water type, state well log ID, latitude and longitude, CRBG formation, depth, sample interval
Field parameters	temperature, specific conductance, pH, redox potential, dissolved oxygen
Bulk chemistry	total dissolved solids, alkalinity, and hardness
Cations	HCO_3^- , CO_3^{2-} , CO_2 , F^- , Cl^- , SO_4^{2-} , SO_2^- , H_2S^-
Anions	CH_4 , NO_3^- , NO_2^- , NH_3 , P^{3-} , PO_4^{3-} , total organic and inorganic nitrogen and carbon
Metals	Li^+ , Al, Fe, Mn
Trace elements	Sb, As, Ba, Be, B, Br, Cd, Cr, Co, Cu, Pb, Hg, Mo, Ni, Rb, Se, Ag, Sr, Tl, U, V, Zn
Stable isotopes	$\delta^2\text{H}$, $^3\text{He}/^4\text{He}$, $\delta^{18}\text{O}$, $\delta^{13}\text{C}$, $\delta^{34}\text{S}$
Radioactive isotopes	^3H , ^{14}C , ^{222}Rn , ^{224}Ra , ^{226}Ra , ^{228}Ra
Radiological measurements	Alpha and beta particles

to Vienna Standard Mean Ocean Water (VSMOW) for $\delta^2\text{H}$ and $\delta^{18}\text{O}$, Vienna Pee Dee Belemnite (VPDB) for $\delta^{13}\text{C}$.

Data analysis

Visual trends were investigated by generating scatterplots of sample depth, field measurements, and dissolved ions. All ion data presented in units of mass per volume (for example, mg/L) were converted to molar concentration (mmol/L) or equivalents (meq/L) for comparative analyses and three outliers from deep oil and gas exploration wells were excluded from further analysis due to unreliable data quality. The scatterplots also include derivative results, such as dissolved ion combinations like a Chadha diagram (Fig. 5). Piper and Durov diagrams that assess the proportional contribution of dissolved ions to total dissolved solids were generated using Geochemists Workbench (Bethke, 2008). This software was also used to calculate mineral saturation states, utilizing both the Lawrence Livermore National Laboratory thermodynamic database (Johnson and others, 2000) for silicates and the Carfix thermo-database (Aradóttir and others, 2012) for carbonate minerals, which contain thermodynamic data for mineral assemblages most relevant to the CRBG.

Summary statistics, principal component analysis (PCA), and hierarchical cluster analysis (HCA) were used to investigate linkages between groundwater chemistry, CRBG formation, and spatial distribution of the samples in the Columbia basin. PCA reduces the dimensions of a dataset to more easily determine the primary controls of dataset variability. HCA groups samples into clusters based on some measure of distance between the variables to identify linkages in large datasets. Combining PCA with HCA helps determine which variables exert the most influence on the distribution of groundwater chemistry.

PCA and HCA were conducted in R, using the “prcomp” and “cluster” packages (University of Cincinnati, 2018). Both scripts require exclusion of samples with missing and non-detect data from the analysis. The PCA was conducted first, to

determine the principal components. Through an iterative process (e.g., stepwise reduction of analytes to narrow the PCA to the smallest number of analytes that lead to the best statistics), the number of useable samples for robust analysis was reduced from 1,537 samples to 1,305 samples because some samples only included a portion of the analytes. The final PCA identified samples which included data pertaining to alkalinity as well as calcium $[\text{Ca}^{2+}]$, sodium $[\text{Na}^+]$, chlorine $[\text{Cl}^-]$, fluorine $[\text{F}^-]$, sulfate $[\text{SO}_4^{2-}]$, and silica $[\text{Si}]$ concentrations. An HCA was then conducted on the resulting PCA scores. The HCA used an agglomerative clustering approach and Ward's minimum variance method to determine the similarity/dissimilarity between samples. The gap statistic method in "cluster" was used to determine three clusters as statistically optimal (University of Cincinnati, 2018).

RESULTS

The data supplement includes the summary statistics for all analytes. Table 2 includes the summary statistics for analytes relevant to this report—not all analytes from Table 1 are discussed herein (for example, trace elements). The data in this study span 125 years of sample collection in the CRBG aquifer system and include samples across the thickness of the CRBG in the Columbia basin at depths as much as 4,682 m (Table 2). However, the mean depth of the samples is much shallower (333 m). Thus, like other regional syntheses (Bauer and Hansen, 2000; Kahle and others, 2011; Tolan and others, 2009c), observations and interpretations on deeper groundwater in the CRBG are not as robust as for shallower groundwater. Yet, this study includes the most comprehensive compilation of data available thus far.

Analytical groundwater chemistry

Only a few sites have data for every analyte in our dataset, and the accuracy of those data depend on the procedures followed by the reporting entity. As a result, charge balance errors (CBE) range from -71% to +75%, though 87% of samples have a CBE less than $\pm 10\%$ and the mean CBE of all data is 1% (Table 2).

FIELD MEASUREMENTS AND BULK CHEMISTRY

Mean groundwater temperatures in the CRBG aquifer system ($T = 21 \pm 9.7^\circ\text{C}$, $n = 1257$, Table 2) are slightly higher than expected (18.3°C) at the average sample depth using a mean annual surface temperature of 10.2°C in the Columbia basin and a geothermal gradient in continental crust of $2.5^\circ\text{C}/100\text{ m}$. This aligns with results of a statewide assessment of geothermal gradient (Forson and others, 2015) and the known thermal wells and mineral springs in the Yakima Fold and Thrust Belt (Mariner and others, 1982). The Columbia basin is in a backarc setting and filled with relatively young volcanics that might provide a shallow heat source and promote higher rates of heat flux (Kolawole and Evenick, 2023).

CRBG groundwaters are alkaline ($\text{pH} = 8.07 \pm 0.74$, $n = 1409$) with significant dissolved carbonate (Alkalinity = $153 \pm 72\text{ mg/L}$ equivalent CaCO_3 , $n = 1092$; Hardness = $86 \pm 64\text{ mg/L}$ equivalent CaCO_3 , $n = 69$). Groundwaters are slightly reducing ($\text{ORP} = -136 \pm 217\text{ mV}$, $n = 197$), with dissolved oxygen levels that are present but low. The average DO of $3.9 \pm 4.3\text{ mg/L}$ ($n = 650$) is likely biased toward higher values (maximum,

78 mg/L ; Table 2) that far exceed the solubility of oxygen in water. Overall CRBG groundwaters are relatively fresh, with SpC values $\leq 2,900\text{ }\mu\text{S/cm}$ ($n = 1325$) and total dissolved solid (TDS) values $\leq 1,634\text{ mg/L}$ ($n = 1498$) except for three deep oil and gas wells.

CATIONS AND ANIONS

Dissolved silica concentrations $[\text{Si}]$ were measured for almost all samples. $[\text{Si}]$ range widely (mean = $27.7 \pm 14.6\text{ mg/L}$, $n = 1,474$). Most samples from sources that measured total nitrate-nitrite concentration $[\text{TN}]$ were not included because they clearly represented anthropogenic influence. Of those that remain, concentrations have values in the range expected from natural sources (mean = $0.58 \pm 1.5\text{ mg/L}$, $n = 104$). Measurements of fluoride concentration $[\text{F}^-]$ are present in almost all samples (mean = $3.7 \pm 9.2\text{ mg/L}$, $n = 1,455$). Concentrations of lithium $[\text{Li}^+]$, aluminum $[\text{Al}]$, manganese $[\text{Mn}]$, and iron $[\text{Fe}]$ are less common in the dataset (mean = $0.087 \pm 1.0\text{ mg/L}$, $n = 372$; mean = $1.8 \pm 10.5\text{ mg/L}$, $n = 226$; mean = $0.26 \pm 1.4\text{ mg/L}$, $n = 341$; mean = $2.0 \pm 15.5\text{ mg/L}$, $n = 864$). The maximum concentration of these elements ($[\text{Li}^+] = 20.0\text{ mg/L}$, $[\text{F}^-] = 50.7\text{ mg/L}$, $[\text{Al}] = 110\text{ mg/L}$, $[\text{Mn}] = 15.6\text{ mg/L}$, and $[\text{Fe}] = 290\text{ mg/L}$) are significantly elevated above representative groundwater from most sedimentary basins, reflecting the volcanic nature and mineral chemistry of the CRBG.

Of the samples in the dataset, most represent alkaline-earth waters, with the majority of those including $>20\%$ molar contribution of alkalis to the cations (Fig. 5). These samples have total dissolved solid (TDS) concentrations that are generally $<600\text{ mg/L}$ and values of pH that range between 7 and 9 (Fig. 5). The anion composition varies between samples dominated by dissolved carbonate and those samples proportionally dominated by sulfate and chloride. Overall, the sulfate $[\text{SO}_4^{2-}]$ and chloride $[\text{Cl}^-]$ concentrations in the CRBG are low (mean = $38.4 \pm 57.3\text{ mg/L}$, $n = 1401$; mean = $53.6 \pm 273\text{ mg/L}$, $n = 1458$; respectively) compared to bicarbonate $[\text{HCO}_3^-]$ concentrations (mean = $211.8 \pm 639.7\text{ mg/L}$, $n = 422$). Alkaline-earth metal mean concentrations (calcium $[\text{Ca}^{2+}] = 25.6\text{ mg/L} \pm 32.4$, $n = 1463$; magnesium $[\text{Mg}^{2+}] = 13.1 \pm 15.4\text{ mg/L}$, $n = 1388$) are of a similar order of magnitude to the mean concentration of alkali-metals (potassium $[\text{K}^+] = 8.2 \pm 27.6\text{ mg/L}$, $n = 1454$; sodium $[\text{Na}^+] = 69.7 \pm 179.0\text{ mg/L}$, $n = 1474$). Thus, on a Chadha diagram (Fig. 6), the bulk of samples are split between the alkaline-earth (right) and alkali quadrants (left) of the carbonate-dominated regime (top). On the Durov diagram (Fig. 5) this is shown as the result of chemical weathering by a combination of dissolution (diagonal trend) and ion exchange (vertical trend). Most remaining samples on the Chadha diagram trend toward the lower left quadrant (Fig. 6) where ion exchange processes indicate highly evolved saline brines enriched in alkalis. A few samples are alkaline-earth waters in the lower right quadrant enriched in sulfate or chloride that likely have some influence by anthropogenic sources not identified during database construction.

STABLE AND RADIOACTIVE ISOTOPES

The stable isotopes of water in CRBG groundwater (mean values of $\delta^2\text{H} = -132.0 \pm 11.9\text{‰}$ and $\delta^{18}\text{O} = -17.0 \pm 1.7\text{‰}$,

Table 2. Summary statistics for select analytes in the database.

Parameter	Measurements*	Minimum	Maximum	Range	Median	Mean	Std. Dev.
Field Parameters							
Well depth (ft)	1,481	18	15,362	15,344	709	1,090	1355
Collection date	1,496	9/16/1916	3/20/2024	N/A	8/13/1982	5/27/1980	N/A
Temperature (°C)	1,257	3	63.9	60.9	19.1	20.80	9.69
SpC (µS/cm)	1,325	0.227	2,900	2,899.8	378	512.33	399
pH	1,409	5.59	10.8	5.21	8	8.07	0.74
ORP (mV)	197	-450	387	837	-202.5	-135.52	217
DO (mg/L)	650	0	77.85	77.85	3.4	3.91	4.33
Bulk Chemistry							
TDS (mg/L)	1,498	14	14,741	14,727	275	381	639
Alkalinity (mg/L as CaCO ₃)	1,092	40	1070	1030	142.62	153.33	71.6
Hardness (mg/L as CaCO ₃)	69	2.5	260	257.5	77	86.31	63.7
CBE (%)	1,301	-71%	75%	146%	2%	1%	10%
Cations							
Calcium (mg/L)	1,463	0	740	740	20	25.6	32.4
Magnesium (mg/L)	1,388	0	120	120	9.8	13.1	15.4
Potassium (mg/L)	1,454	0.1	739	738.9	6.2	8.21	27.6
Sodium (mg/L)	1,474	2	4,410	4,408	36	69.7	179
Anions							
Bicarbonate (mg/L)	422	22	13,000	12,978	161	211.8	639.67
Chloride (mg/L)	1,458	0	7392	7,392	10	53.63	272.99
Fluoride (mg/L)	1,455	0.053	50.8	50.75	0.6	3.69	9.20
Total nitrate-nitrite (mg/L)	104	0.071	8.1	8.029	0.125	0.58	1.47
Sulfate (mg/L)	1,401	0	720	720	21	38.39	57.34
Silica (as Si, mg/L)	1,474	0	140	140	24.3	27.7	14.59
Metals							
Lithium (ug/L)	372	0	20,000	20,000	20	86.79	1038
Aluminum (mg/L)	226	0.0007	110	110	0.080	1.848	10456
Iron (mg/L)	864	0	290	290	0.050	1.97	15463
Manganese (mg/L)	341	0	15.6	15.6	0.020	0.255	1418
Isotopes							
δ ² H (‰ - VSMOW)	210	-152.3	-93.6	58.7	-133	-132	11.86
δ ¹⁸ O (‰ - VSMOW)	201	-19.5	-4.2	23.7	-17.2	-17.0	1.65
δ ¹³ C (‰ - VPDB)	168	-44.1	20.7	64.8	-12.2	-11.7	6.91
δ ³⁴ S (‰ - VCDT)	41	-6	36.2	42.4	11.2	14.7	11.39
¹⁴ C (pmc)	117	0.18	110	109.8	17.7	31.6	30.19

*The number of measurements vary because not all samples were measured for every analyte.

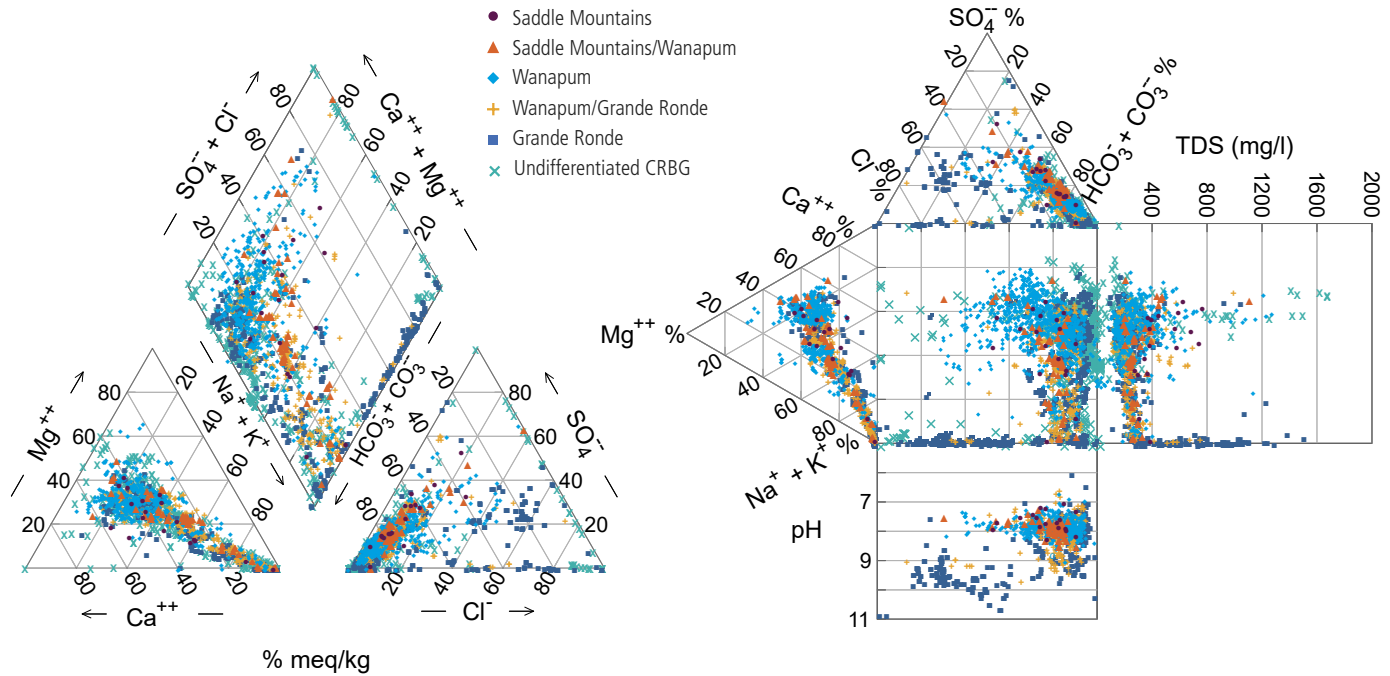


Figure 5. Piper (left) and Durov (right) diagrams showing the proportional abundance of principal cations and anions in groundwaters from the Columbia River Basalt Group. The colors and shapes indicate the listed formation at the sampling depth. Samples from greater depths in the Grande Ronde Basalt have high $[\text{Na}^+]$, $[\text{Cl}^-]$, and pH and form a distinct group on both plots.

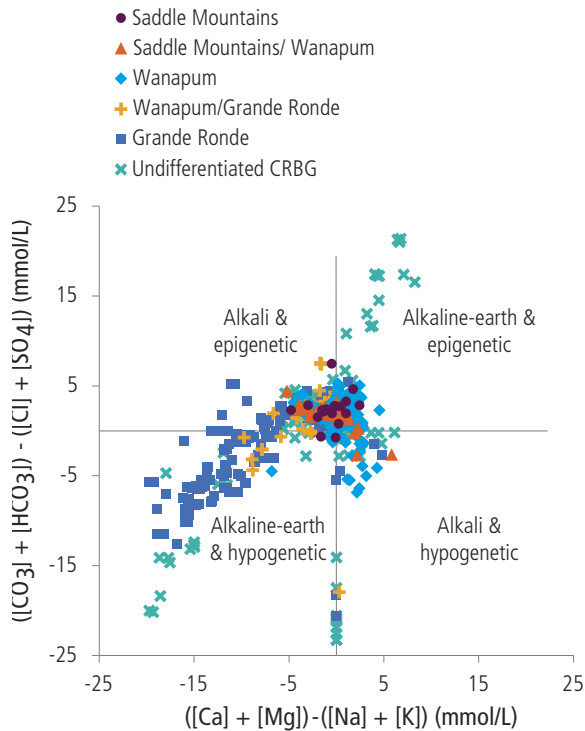


Figure 6. Chadha Plot of groundwater samples from the Columbia River Basalt Group that shows the sum of alkaline-earth metals minus the sum of alkali metals on the x axis and the carbonate species minus the sum of chloride and sulfate on the y axis. All four quadrants are labeled with a short description of water type. Epigenetic refers to surficial processes guiding reactions between meteoric recharge and the basalt. Hypogenetic refers to deep aquifer processes isolated from meteoric recharge. The colors are classified by listed formation at the sampling depth. Samples from deeper in the Grande Ronde Basalt have elevated $[\text{Na}^+]$ and $[\text{Cl}^-]$ and trend toward saline waters in the lower left quadrant of the diagram.

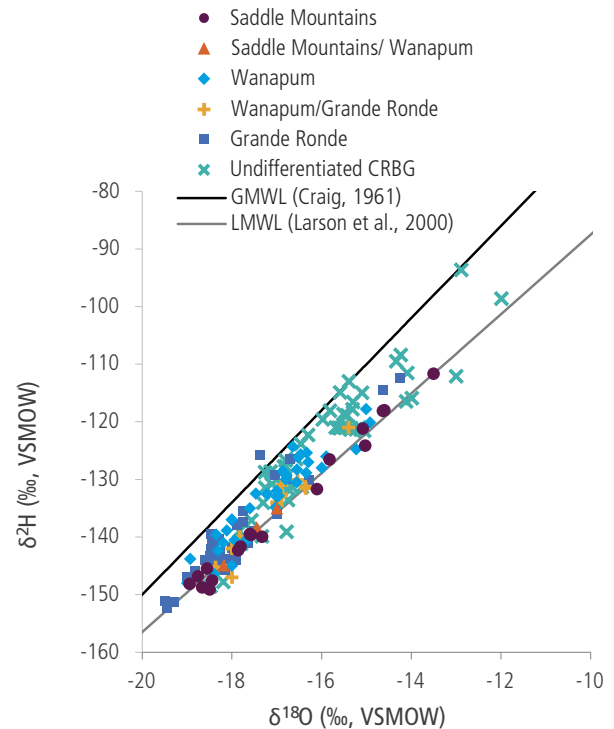


Figure 7. Scatterplot showing the $\delta^{18}\text{O}$ and $\delta^2\text{H}$ of groundwaters in the Columbia River Basalt Group, classified by listed formation at the sampling depth. Included are the local meteoric water line (LMWL) obtained by Larson and others (2000) and the global meteoric water line (GMWL) of Craig (1961) from deeper in the Grande Ronde Basalt have elevated $[\text{Na}^+]$ and $[\text{Cl}^-]$ and trend toward saline waters in the lower left quadrant of the diagram.

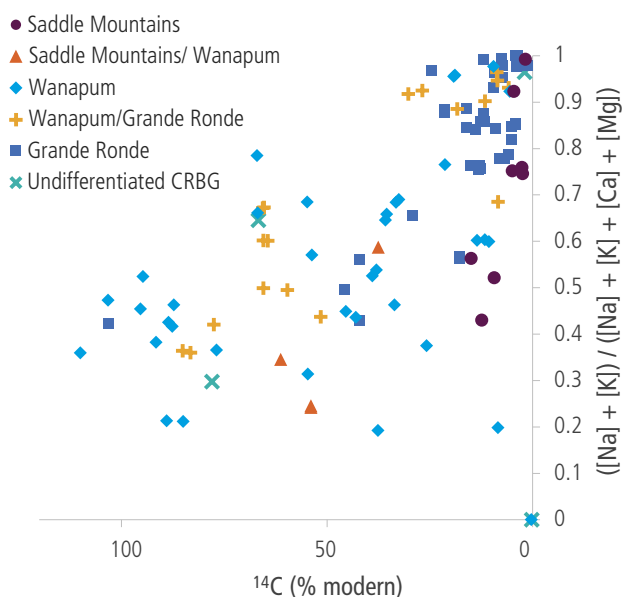


Figure 8. Scatterplot showing the variation of cation ratio $([\text{Na}] + [\text{K}]) / ([\text{Na}] + [\text{K}] + [\text{Ca}] + [\text{Mg}])$ as a function of ^{14}C (in % modern) in groundwaters from the Columbia River Basalt Group, classified by listed formation at the sampling depth.

$n = 201$) are more depleted than measurements from precipitation in the Columbia basin (mean value of $\delta^{18}\text{O} = -15.9$; Robertson and Gazis, 2006). Water is slightly more depleted in the heavier isotopes in samples west of the Columbia River (as much as $\delta^2\text{H} = -152.3$ ‰ and $\delta^{18}\text{O} = -19.5$ ‰) and slightly less depleted in samples east of the Columbia River (as little as $\delta^2\text{H} = -112.1$ ‰ and $\delta^{18}\text{O} = -13.0$ ‰). The collected data follow linear regressions (Fig. 7) that lie between the global meteoric water line (GMWL; $\delta^2\text{H} = 8 \times \delta^{18}\text{O} + 10$; Craig, 1961) and the local meteoric water line modeled from precipitation in the Columbia basin (LMWL; $\delta^2\text{H} = 6.9 \times \delta^{18}\text{O} - 18.5$; Larson and others, 2005). Namely, samples specifically from the Saddle Mountains Basalt plot along the LMWL ($\delta^2\text{H} = 7.1 \times \delta^{18}\text{O} - 15.6$, $r^2 = 0.99$), while wells completed in the underlying Wanapum Basalt ($\delta^2\text{H} = 6.9 \times \delta^{18}\text{O} - 14.7$, $r^2 = 0.89$), the Grande Ronde Basalt ($\delta^2\text{H} = 7.5 \times \delta^{18}\text{O} - 5.6$, $r^2 = 0.88$), and the undifferentiated samples from springs and oil and gas wells ($\delta^2\text{H} = 7.5 \times \delta^{18}\text{O} - 4.3$, $r^2 = 0.87$) plot closer to the GMWL.

Stable isotopes of inorganic carbon in CRBG groundwater have values ($\delta^{13}\text{C} = -11.7 \pm 6.9$ ‰, $n = 168$) that are between values expected from marine carbonates (0 ‰ ± 5 ‰; Faure, 1986), dry-adapted C4 vegetation (-10 ‰ to -16 ‰; Farquhar and others, 1989), and Cenozoic carbon dioxide in the atmosphere (-8.5 ‰ to -4 ‰; Tipple and others, 2010). East of the Columbia River, sample $\delta^{13}\text{C}$ values are less dispersed; west of the Columbia River some samples are highly depleted in the heavier isotope (as low as $\delta^{13}\text{C} = -44.1$ ‰) and others are highly enriched in the heavier isotope (as great as $\delta^{13}\text{C} = +20.7$ ‰).

Stable isotopes of sulfur in CRBG groundwater have values (mean value of $\delta^{34}\text{S} = +14.7 \pm 11.4$ ‰, $n = 41$) that are more depleted in the heavier isotope than values from Miocene seawater ($\delta^{34}\text{S} = +21$ ‰ to $+23$ ‰; Paytan and others, 1998) and less depleted than values expected from basalt ($\delta^{34}\text{S} = -8$ ‰ to $+6$ ‰). Like the other stable isotopes, values in the database have different distributions east versus west of the Columbia River.

West of the Columbia River, samples are generally more depleted in the heavier isotope (as low as $\delta^{34}\text{S} = -6$ ‰). East of the river, samples have a much greater variation and are generally more enriched in the heavier isotope (as great as $\delta^{34}\text{S} = +36.2$ ‰).

Radioactive carbon values in CRBG groundwater range from ancient ($>50,000$ years) to modern ($^{14}\text{C} = 0.18$ ‰ to 110 ‰ pmc) and do not appear to have a clear east-to-west component to their distribution. Rather, there is a trend toward older groundwaters in deeper samples that have greater ratios of the concentrations of alkali metals $[\text{Na}^+ + \text{K}^+]$ to total cations $[\text{Na}^+ + \text{K}^+ + \text{Ca}^{2+} + \text{Mg}^{2+}]$; samples with >80 ‰ of their cations composed of sodium and potassium have <20 ‰ pmc of ^{14}C (Fig. 8).

Spatial variation in groundwater chemistry

The data supplement includes scatterplots of all relevant analytes in the dataset. A few were introduced in the previous discussion on isotope geochemistry (Figs. 7 and 8). The remainder support the following generalized statements: (1) Intra- and inter-formation groundwater chemistry varies significantly in the CRBG with evidence of depth specific trends, (2) the concentration of dissolved carbonate is inversely proportional with salinity and pH, and (3) the concentration of alkali metals is inversely proportional with that of alkaline earth metals.

SELECTED COMPARISONS WITH FORMATION AND DEPTH

CRBG formations are sub-horizontal and, as such, there are many correlations in the scatterplots between depth of sample and formation across the Columbia basin. Post-emplacement deformation has resulted in a wide elevation range of CRBG formation outcrops. For example, outcrops of the top of the Grande Ronde Basalt vary from elevations $>1,950$ m on Table Mountain north of Ellensburg to <100 m on the banks of the Columbia River near The Dalles. As such, samples identified from the Grande Ronde Basalt span depth ranges from those at the surface of the basin margins to depths $>1,300$ m in the center of the basin. The deepest samples from oil and gas wells typically do not have flow member interpretations as they mainly targeted sub-basalt units.

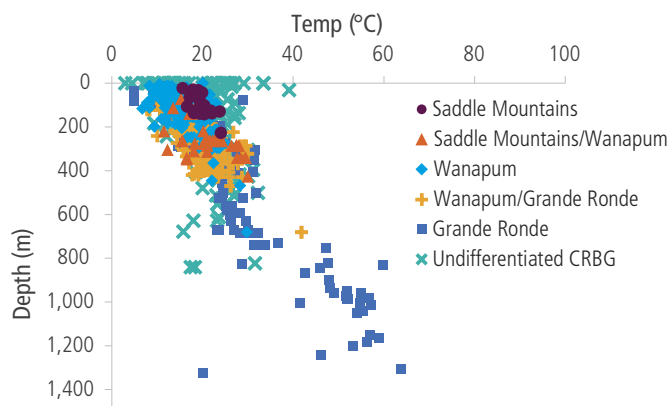


Figure 9. Scatterplot comparing temperature with depth in Columbia River Basalt Group groundwater, classified by listed formation at the sampling depth.

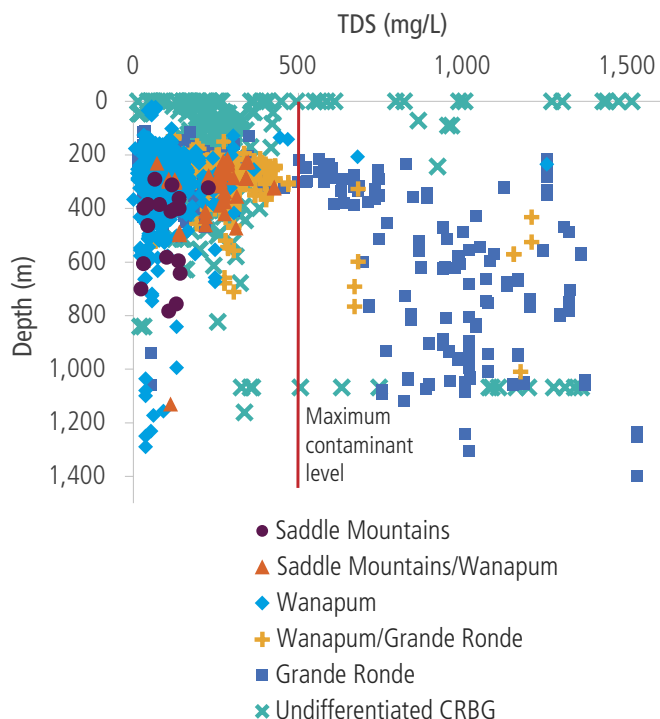


Figure 10. Scatterplot comparing the concentration of total dissolved solids (TDS) with depth in Columbia River Basalt Group groundwater, classified by listed formation at the sampling depth. The red line indicates the published maximum contaminant level (MCL) for TDS.

The geothermal gradient computed from groundwater samples from the Grande Ronde Basalt is ~ 4.0 °C/100 m ($T = 3.95 \times D + 10.13$, $r^2 = 0.87$; Fig. 9), which further illustrates an elevated heat flux compared to sedimentary basins. However, the temperature of samples increases significantly (~ 15.0 °C) at depths of 650 to 750 m, such that the gradient more accurately comprises two linear functions with slope of approximately 3.2 °C/100 m separated by a zone where the temperature increases at a greater rate. There appears to be a vertical barrier to heat flux in at least some portion of the Columbia basin.

Values of TDS and SpC have a bimodal distribution with respect to depth in the dataset (Fig. 10) as do many of the dissolved cations and anions. For TDS, samples that exceed the 500 mg/L maximum contaminant level (MCL) (EPA, 2024) are from all CRBG formations at depths of less than 350 m and from depths greater than 650 meters that are mostly in the Grande Ronde Basalt. The samples between 350 m and 650 m largely have SpC values less than 500 $\mu\text{S}/\text{cm}$.

Some of the samples from the Wanapum Basalt have TDS as high as 1,300 mg/L, and some mineral springs have TDS as high as 1,700 mg/L. Samples from the Grande Ronde Basalt (including those samples that likely have a mix of groundwater from the Wanapum and Grande Ronde basalts) are either alkaline-earth waters (Ca-Mg- HCO_3^- type) or alkaline waters with varying $[\text{HCO}_3^-]$ to $[\text{Cl}^-] + [\text{SO}_4^{2-}]$ ratios (Fig. 5). The alkaline-water Grande Ronde samples have the highest TDS reported from wells in the dataset ($>1,500$ mg/L), with pH of between 9 and 11. Some of the samples in this category represent Na- HCO_3^- type groundwater. The other, smaller subset in this category is Na-Cl-type groundwaters from deep oil and gas wells (Fig. 5).

The samples with high TDS and SpC at depths <350 m fall into two categories: mineralized waters emerging from

springs at outcrop that likely tap a deeper source, and samples from wells located in agricultural areas and downgradient of irrigation canals. The first category includes many carbonate-enriched (soda) springs in the western basin margin that degas carbon dioxide and have alkalinity >5 meq/L CaCO_3 , $[\text{HCO}_3^-] >10$ mmol/L, and $[\text{Ca}^{2+}] >2$ mmol/L. The second category is from the Saddle Mountains and Wanapum basalts in the central basin and likely have anthropogenic influence, with $[\text{TN}] >2$ mmol/L, $[\text{Cl}^-] >5$ mmol/L, and $[\text{SO}_4^{2-}] >2$ mmol/L. For the samples deeper than 650 m, many are enriched in Cl^- (≤ 21.2 mmol/L), F^- (≤ 2.7 mmol/L), and Na^+ (≤ 19.6 mmol/L).

The TDS and SpC, as with groundwater temperature, increase markedly between 650 and 750 m, driven by major increases in $[\text{Cl}^-]$, $[\text{F}^-]$, $[\text{Na}^+]$, and $[\text{Al}]$. Inversely, $[\text{Ca}^{2+}]$ and $[\text{Mg}^{2+}]$ decrease from the surface to near zero concentrations at depths >650 m. At the same time, neutral pH values at the surface increase to an asymptote of 9.5 at depths below 750 m. These observations again point to a division between shallower and deeper groundwater chemistry that could be the result of a barrier to vertical groundwater mixing.

The samples from depths >750 m have a range of groundwater chemistry but are generally more mineralized than shallower waters. Samples that are less mineralized at depth are likely from the basin periphery and the more mineralized deeper samples are from the central basin. The more mineralized deeper samples are alkaline (pH >9.5), but anoxic ($[\text{DO}] \approx 0$ mg/L) and highly reducing (ORP <-200 mV), with elevated salinity ($[\text{Cl}^-]$ and $[\text{Na}^+] >5$ mmol/L), sulfate ($[\text{SO}_4^{2-}] >1$ mmol/L), and dissolved metals ($[\text{Al}] >0.01$ mmol/L). The samples with TDS $>1,000$ mg/L are brackish groundwaters; however, and importantly, only three samples in the dataset are saline with TDS $>10,000$ mg/L.

Groundwaters in the Grande Ronde Basalt at depths >650 m are late Pleistocene (pmc $<0.2\%$ or >20 kybp). Shallower waters between the surface and 650 m depth have a large scatter in ^{14}C ages but generally become older with depth. Both $\delta^2\text{H}$ and $\delta^{18}\text{O}$ trend toward more depletion in the heavier isotope between the surface and depths of 650 m. Below 650 m, measurements of $\delta^{18}\text{O}$ are limited. Values of $\delta^2\text{H}$ below 650 m have increased scatter with some samples as enriched in the heavier isotope as those from surface samples. In contrast, $\delta^{13}\text{C}$ values are more tightly clustered about the mean at depths <650 m. At depths >650 m, $\delta^{13}\text{C}$ values include those that are highly enriched and highly depleted in the heavier isotope. Values of $\delta^{34}\text{S}$ are the reverse of carbon isotopes in that samples at depths <650 m are more enriched in the heavier isotope with a larger range, and the samples at depths >650 m are more depleted in the heavier isotope with less spread in the values.

SELECTED COMPARISONS BETWEEN ANALYTES

Despite scatter, there is a 1:1 linear relationship between $[\text{Ca}^{2+}]$ and $[\text{Mg}^{2+}]$ across the CRBG formations. Some mineral springs and deeper, undifferentiated wells have proportionally more Mg^{2+} than Ca^{2+} in solution. The concentrations of the alkaline-earth metals are generally not the product of the carbon or sulfur pathways for the carbonate equilibrium reactions in a closed system except at concentrations of $[\text{Ca}^{2+}] + [\text{Mg}^{2+}] <1$ mmol/L and $[\text{HCO}_3^-] <2$ mmol/L, where the proportionality is close to 1:2.

There is considerable scatter in the relationship between $[\text{Na}^+]$ and $[\text{K}^+]$. Most data do not fall below a proportionality of

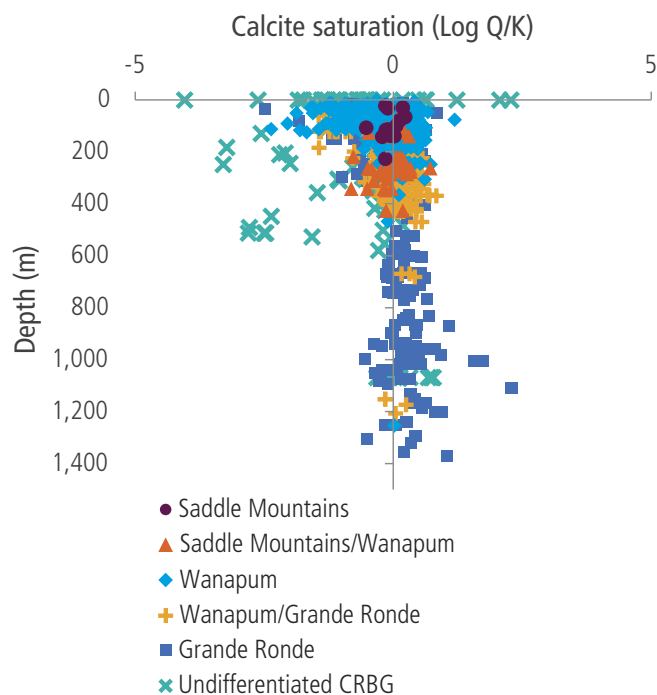


Figure 11. Scatterplot comparing calcite saturation index (SI) with depth in Columbia River Basalt Group groundwater, classified by listed formation at the sampling depth. Values of SI > 0 indicate the mineral can precipitate, while values of SI < 0 indicate the mineral can dissolve.

~6:1, which is in line with the general abundance of sodium versus potassium in basalt. Because potassium is readily incorporated into secondary minerals, one subset of Grande Ronde Basalt samples are clustered around a proportionality of ~25:1 and a second subset cluster around a proportionality of ~100:1. The increasing concentrations of alkali metals across all CRBG formations outpace the increase in $[Cl^-]$ by 2:1 in samples with $[Cl^-] < 10$ mmol/L. The exceptions are wells that have anthropogenic influence. In samples with $[Cl^-] > 10$ mmol/L, the trend decreases to a proportionality close to 1:2.

The concentration of Na^+ at depth surpasses even the highest Ca^{2+} concentrations in the dataset. As a result, the comparison of alkaline-earth metals to alkali metals shows no proportional increase in $[Ca^{2+}] + [Mg^{2+}]$ where the $[Na^+] + [K^+] > 5$ mmol/L. This is better shown in the Piper and Durov diagrams of Figure 5 and in the comparison of the alkaline-earth metals to the ratio of alkalis to total cations where the scatter in and sum of $[Ca^{2+}] + [Mg^{2+}]$ is inversely proportional with increasing $[Na^+ + K^+] / [Na^+ + K^+ + Ca^{2+} + Mg^{2+}]$. In contrast $[Na^+]$, $[Cl^-]$, $[F^-]$, and pH all increase with increasing ratio of alkali metals to total cations, suggesting that the deeper groundwaters with elevated levels of these analytes are more highly evolved.

At $[Cl^-] < 2$ mmol/L there is a direct proportionality with $[HCO_3^-]$ in solution. However, at $[Cl^-] > 2$ mmol/L, this trend diminishes, and may even show a slight inverse proportionality. Rather, the samples with higher $[Cl^-]$ tend to have lower $[HCO_3^-]$, although limited measurements of $[HCO_3^-]$ at depth prevent robust observations. The relationship between $[SO_4^{2-}]$ and $[Cl^-]$ is more complicated. Some deeper samples from the Grande Ronde Basalt and undifferentiated mineral springs and deep wells have almost exclusively Cl^- compared to SO_4^{2-} . Another set of Grande Ronde Basalt samples have a $[SO_4^{2-}]$ to $[Cl^-]$

proportionality of 2:5. Remaining samples from the Grande Ronde, Wanapum, and Saddle Mountains basalts are scattered above the 2:5 proportionality of $[SO_4^{2-}]$ to $[Cl^-]$.

The limited number of $[PO_4^{3-}]$ and $[P^{3-}]$ measurements limit any inferences about the connections between $[F^-]$ and the dissolution of fluorapatite, although samples with elevated $[F^-]$ are also elevated in $[P^{3-}]$. Finally, the relationships between $[Cl^-]$ and $[Na^+]$ compared to $[F^-]$ follow similar patterns and illustrate trends in the samples: (1) a grouping with $[F^-] < 0.2$ mmol/L that represent shallow wells with variable $[Cl^-]$ and $[Na^+]$ based on the magnitude of anthropogenic input, (2) a grouping with $[F^-] < 0.2$ mmol/L and the highest $[Cl^-]$ and $[Na^+] > 14$ mmol/L that represent deep wells in the Grande Ronde Basalt or undifferentiated oil and gas wells, (3) a set of samples from the Grande Ronde Basalt that have a proportional increase in $[F^-]$ to $[Cl^-]$ of ~1:10; and (4) a second set of samples from the Grande Ronde Basalt that have a greater proportional increase in $[F^-]$ to $[Cl^-]$ of ~4:10. This last grouping comes from depths that are on average deeper than the third group, although no tests of independence were conducted to see if these groups were independent populations.

Modeled groundwater chemistry

The data supplement collects plots of all computed saturation indices (SI) for the data in this study, organized by CRBG formation and by depth. Groundwater in the Saddle Mountain and Wanapum basalts, largely from shallow wells at cooler temperatures, is typically undersaturated with respect to calcite. In contrast, deeper and warmer samples from the Grande Ronde Basalt are typically oversaturated with respect to calcite (Fig. 11). However, it is important to note the significant measurement

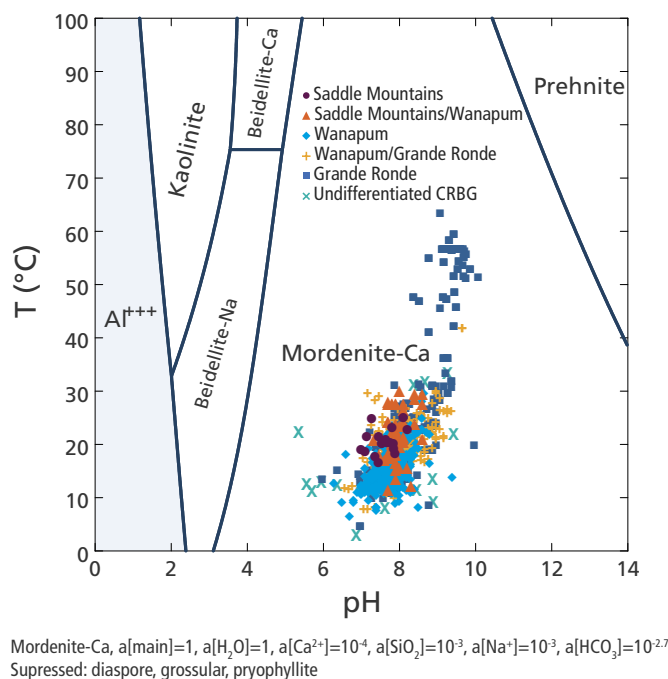


Figure 12. Diagram depicting the mineral stability fields relative to calculated ion concentrations and activity ratios in Columbia River Basalt Group groundwater, classified by listed formation at the sampling depth. All samples in the database are stable with respect to mordenite, a form of zeolite.

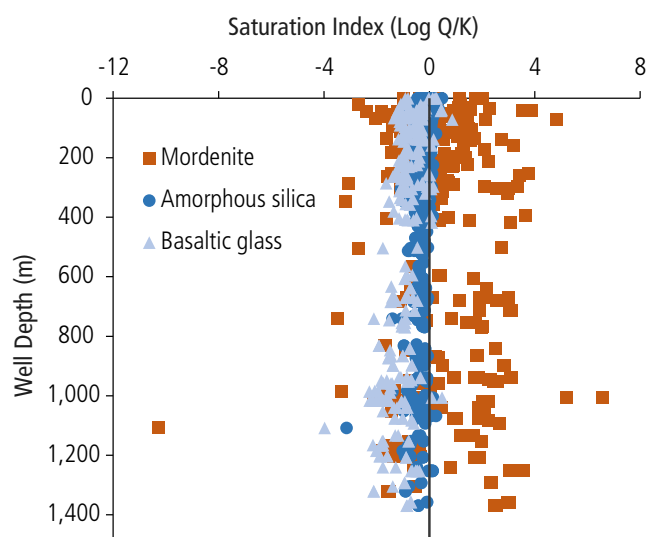


Figure 13. Scatterplot comparing the saturation index (SI) with depth for mordenite (a zeolite), amorphous silica, and basaltic glass. Values of $SI > 0$ indicates the mineral can precipitate, while values of $SI < 0$ indicates the mineral can dissolve.

errors possible in both alkalinity and pH and the possibility that many deeper wells are open across multiple flow units, co-mingling waters from multiple flow units.

Mineral stability diagrams (Fig. 12) show that most samples in the dataset plot in the stability field for the zeolite aluminosilicate mineral mordenite (a substitute for clinoptilolite that is free of aluminum). Mordenite does not have a trend between SI and formation or depth and samples across the CRBG thickness are slightly oversaturated. Both types of zeolites are found in weathered CRBG outcrops and are presumed to be from secondary mineralization (Deutsch and others, 1982). Amorphous silica and basaltic glass are largely undersaturated, regardless of formation or depth in the CRBG (Fig. 13). Because aluminum does not remain in solution in the pH ranges of most samples, [Al] measurements are low and sparse, which limits the ability to calculate saturation indices for most other aluminosilicate minerals.

Clusters of groundwater chemistry

Table 3 includes the proportion of variance explained (PVE) by each principal component (PC) of the PCA using only samples with complete records ($n = 1305$) for alkalinity, $[Ca^{2+}]$, $[Na^+]$, $[Cl^-]$, $[F^-]$, $[SO_4^{2-}]$, and $[Si]$. The top three PCs explained 85.5 % of the variability in this data subset. The weighting of each analyte for the paired combinations of PC1, PC2, and PC3 are shown in Figure 14. PC1 with a $PVE = 46.0\% \pm 1.8\%$ is characterized by negative loadings of alkalinity and $[Ca^{2+}]$ and positive loadings of $[Na^+]$, $[Cl^-]$, $[F^-]$, $[SO_4^{2-}]$, and $[Si]$. PC2 with a $PVE = 25.1\% \pm 1.3\%$ shows negative loadings for $[Na^+]$ and $[F^-]$, and positive loadings for alkalinity, $[Ca^{2+}]$, $[Cl^-]$, $[SO_4^{2-}]$, and $[Si]$. PC3 with a $PVE = 14.4\% \pm 1.0\%$ is negatively loaded for alkalinity and $[Si]$. $[Na^+]$ is essentially zero weighted. $[SO_4^{2-}]$ has strong positive loading, while $[Ca^{2+}]$, $[Cl^-]$, and $[F^-]$ have less positive loading.

The hierarchical cluster analysis on the PCA scores identified 3 statistically significant groups. (Fig. 15). Group 1 comprises most wells across all CRBG formations and has lower average weighting on each PC. This group of samples tends to lean toward Ca-Mg- HCO_3 -type groundwaters that are SO_4^{2-} poor, with consistent $[Si]$ and variable $[Na^+]$ and $[Cl^-]$. Group 2 samples are characterized by Na-Cl-type groundwaters with consistent $[Si]$, depleted alkalinity and $[Ca^{2+}]$, and elevated $[F^-]$. These samples represent wells completed in Grande Ronde Basalt below 650 m. Group 3 includes the remaining samples from

Table 3. The proportion of variance explained by each principal component.

Principal Component	Standard Deviation	Proportion of Variance Explained (%)	Cumulative Variance Explained (%)
1	1.795	46.03	46.03
2	1.325	25.09	71.12
3	1.003	14.38	85.50
4	0.677	6.54	92.04
5	0.610	5.31	97.35
6	0.402	2.31	99.66
7	0.152	0.33	99.99

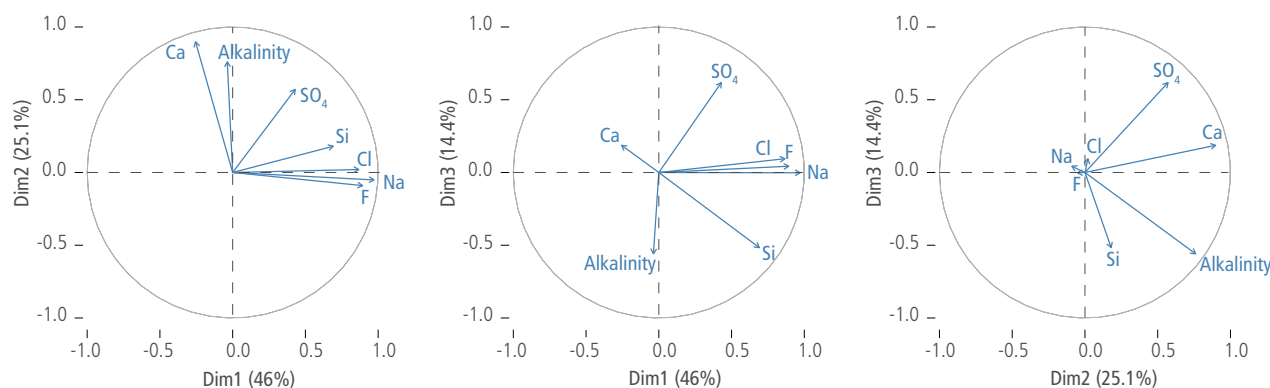


Figure 14. Plots from principal component analyses (PCA) that show the eigenvector weighting of each variable for PC1, PC2, and PC3. The percent of variance accounted for by each eigenvalue is given on the axis.

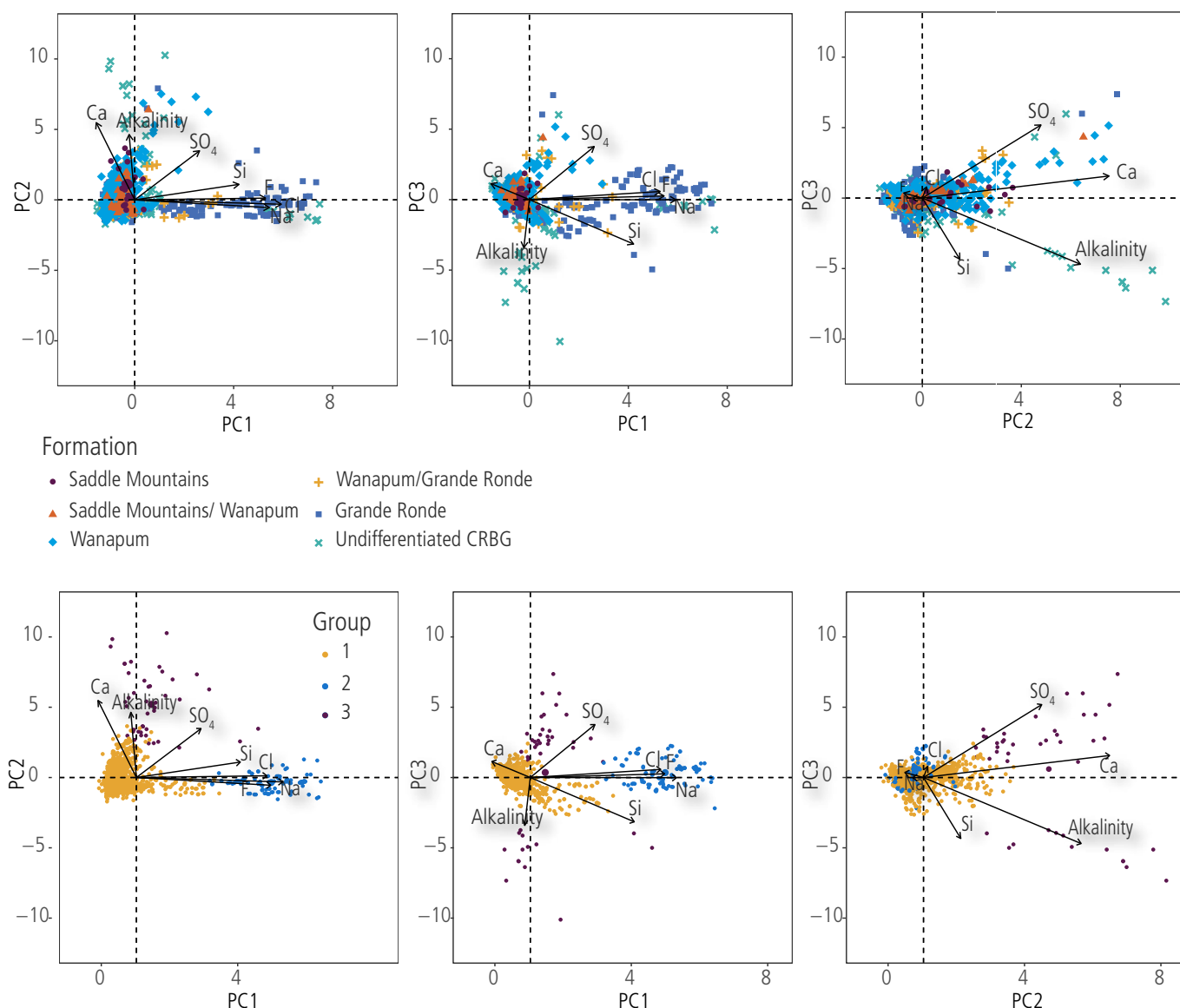


Figure 15. Scatterplots of Columbia River Basalt Group groundwaters on the results of the principal component analysis. At top, the samples are classified by listed formation at the sampling depth. At bottom, the samples are classified by groups identified in the hierarchical cluster analysis.

<350 m deep that have elevated TDS in two categories: the first trend toward Ca-Mg-SO₄-type groundwaters in the Wanapum Basalt that have low [Na⁺], [Cl⁻], and [F⁻], and the second are Ca-Mg-HCO₃-type groundwaters from mineral springs and wells that are highly alkaline.

DISCUSSION

The groundwater chemistry in the Columbia River Basalt Group of the Columbia basin is a story of meteoric waters undergoing water-rock interactions along long flow paths. In this reporting of the most comprehensive database of groundwater chemistry for the Columbia basin to date, we provide a robust analysis of 26 analytes for the 1,537 individual samples in the database. Our findings align with conclusions of prior work.

The overarching messages from this work are as follows. Aquifer recharge is focused in the highlands around the basin periphery. Aquifer discharge occurs in a semi-arid setting along the deeply incised canyons of the Columbia and Snake rivers

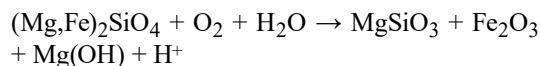
and their tributaries. In the center of the basin, where the basalt thickness exceeds 3,000 m, the portions of the CRBG aquifer below river grade are relatively stagnant because the vertical movement of groundwater is limited due to the stacked architecture of the basalt flows, which includes laterally contiguous zones of both high and low permeability. As such, these deeper groundwaters are warmer and chemically more evolved through weathering of the basalt. Even so, deep groundwater in the CRBG is nowhere mineralized to the point of being considered saline (TDS ≤ 1,700 mg/L). While this makes the CRBG aquifer system suitable for use as a source of potable and irrigation water even at depth, the freshness of the deep groundwater may limit the feasibility for carbon sequestration, enhanced geothermal, and thermal energy storage projects under the current regulatory framework that requires TDS > 10,000 mg/L.

In this discussion, we will consider the groundwater geochemistry of the CRBG aquifer system through the following lenses: (1) the key geochemical reactions that guide the chemistry and their implications for groundwater flow, (2) the vertical

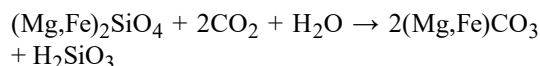
stratification of CRBG groundwater, and (3) the spatial variation in CRBG groundwater. As is common with these discussions, these topics cannot be considered in isolation.

Primary controls on CRBG groundwater chemistry

The chemical composition of groundwater in the Columbia basin is largely the result of mineral reactivity. Near surface, both oxidation and carbonation reactions occur with meteoric waters. For example, olivine (forsterite-fayalite) in basalt may oxidize to form enstatite, hematite and magnesium hydroxide, with a free proton, or:

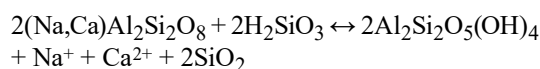


Similarly, olivine may react with carbon dioxide to form a blend of magnesite and siderite with silicic acid, or:

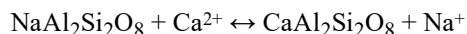


The mean $\delta^{13}\text{C}$ of dissolved inorganic carbon (Table 2) demonstrates a carbon source in most samples that is a blend of CO_2 sourced from the atmosphere and the decomposition of C4 vegetation.

The above forward reactions generate additional acidity that can continue to weather other basalt minerals into a suite of alteration products (Fig. 3). These further reactions result in the release of significant silica and cations in solution (Table 2). For example, plagioclase (albite-anorthite) feldspar may undergo hydrolysis in the presence of silicic acid to produce kaolinite and release calcium, sodium, and free silica into solution, or:



As dissolved oxygen and CO_2 are consumed, pH levels increase and carbonate minerals precipitate. Chemical weathering in these reducing (ORP < 0) parts of the CRBG may occur via slower-acting ion-exchange reactions. For example, dissolved calcium may substitute for the sodium in plagioclase, transforming albite to anorthite and increasing $[\text{Na}^+]$ in solution at the expense of $[\text{Ca}^{2+}]$.



However, the pace of these reactions are slow at the observed temperatures in the samples. Increasing temperatures and pressures with depth amplify the solubility of silicate minerals while decreasing the solubility of carbonates. Deeper waters are therefore depleted in the alkaline-earth metals (Ca^{2+} , Mg^{2+}) by carbonate precipitation while enhanced in the alkali metals (Na^+ , K^+) by cation exchange.

The area of available reaction surface is a first-order control on the rate of chemical weathering. Thus, the vesicular flow tops and brecciated flow bases, with their high porosity, along with fracture apertures are the focus of weathering reactions. Pillow-palagonite facies with highly reactive basaltic glass and associated flow margins is most likely one major control on

TDS in CRBG groundwaters (Steinkampf and others, 1985; Steinkampf and Hearn, 1996).

The refresh rate of groundwater is a second-order control on chemical weathering as O_2 , CO_2 , and acidity are rapidly consumed in weathering reactions, and because weathering products in solution limit the capacity for additional dissolved ions. Since carbonate equilibrium reactions are rapid, CRBG groundwater is only undersaturated with respect to calcite along permeability pathways at shallow depth (Fig. 11). In the semi-arid portions of the Columbia basin, evapotranspiration leads to the formation of carbonate caliche near the surface. Silicate equilibrium and hydrolysis reactions are considerably slower, thus CRBG groundwaters remain undersaturated with respect to silica and basaltic glass even at depth (Fig. 13). Finally, ion exchange reactions between groundwater and minerals are very slow and, while they may occur throughout the aquifer, are more important at depth in older, stagnant groundwaters.

Subaerial exposure time is an important limiting factor on the degree of these weathering reactions. Flow tops that experience extended subaerial exposure may form pedogenic breccias that increase the rate of meteoric recharge, circulation of dissolved oxygen, and the input of organic carbon. Interflow horizons between flows similarly may represent periods of fluvial or lacustrine influence with greater recharge, oxygenation, and carbon input. In particular, the top of the Grande Ronde and Wanapum basalts are notable for long periods of subaerial exposure (Reidel and others, 2013).

Samples presented in this study fall into three statistically independent groups (Fig. 15): (1) those in the Saddle Mountains and Wanapum basalts that have been impacted by recharge of agricultural nutrients, (2) those samples across all CRBG formations, enriched in alkaline-earth metals (Ca^{2+} and Mg^{2+}) that are most significantly influenced by oxidation and carbonization reactions by actively circulating groundwater, and (3) samples almost exclusively in the Grande Ronde Basalt that are enriched in alkali metals (Na^+ and K^+) and most directly undergoing cation exchange reactions in relatively stagnant waters. Correlations between these groups include both depth trends and trends related to spatial anisotropy.

Vertical stratification of CRBG groundwater

The most obvious pattern in the CRBG groundwater chemistry data is a variation with depth. Shallow groundwaters are Ca-Mg- HCO_3 -type (Fig. 5) that are oxidizing with near-neutral pH. Deep groundwaters are Na-Cl-type (Fig. 5) that are reducing and alkaline. The transition between these two end member water types is progressive but not gradational—there is an abrupt change across most analytes at depths between 650–750 m (for example Figs. 9 and 10). The alkaline earth metals are the most abundant cations at shallow depths across all CRBG formations, and gradually reduce in proportion to total cations in deeper wells (Fig. 16). At depths >750 m in the Grande Ronde Basalt the alkali metals constitute almost 100% of the cations in solution.

The increasing proportion of alkali metals with depth follows observations by Steinkampf and Hearn (1996), who noted that $[\text{Na}^+]$ in CRBG groundwater exceeds the abundance of sodium in basaltic glass and suggest that sodium is

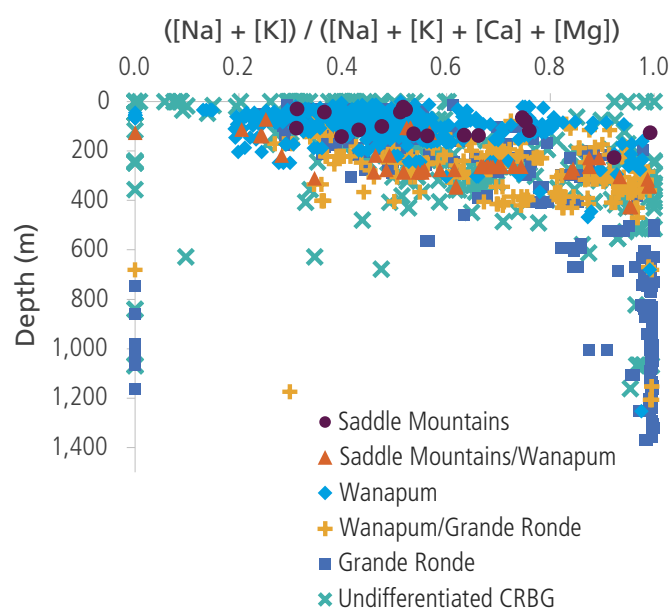


Figure 16. Scatterplot comparing the cation ratio $([Na] + [K]) / ([Na] + [K] + [Ca] + [Mg])$ as a function of depth in groundwaters from the Columbia River Basalt Group, classified by formation.

conserved in solution and can be used as an indicator of the extent to which groundwater has evolved. They further correlated $[Na^+]$ with ^{14}C to determine three different rates of increase of Na in groundwater. Vlassopoulos and others (2012) were similarly able to correlate groundwater ^{14}C age with the ratio of alkalis to total cations $([Na] + [K] / [Ca] + [Mg] + [Na] + [K])$ as another proxy for groundwater evolutionary extent. This report, which includes data from these earlier studies, results in the same expected trend: samples with increasing proportion of alkali metals are more chemically evolved and are at least Pleistocene in age ($pmc < 20\%$, Fig. 8). These older groundwaters include, but are not exclusive to, samples from depths >750 m from the Grande Ronde Basalt that have greater average $[Si]$, $[Al]$, $[P^{3-}]$, $[Cl^-]$, $[F^-]$, and $[SO_4^{2-}]$. This is expected for groundwaters more chemically evolved from interactions with mineral phases in tholeiitic basalt, including sulfides such as pyrite, phosphates like chloro-fluoro-apatite, and aluminosilicates like plagioclase, augite, and biotite.

The geochemistry data reveal a distinction between an upper and lower CRBG aquifer that is regionally present in the Columbia basin. The temperature profile with depth (Fig. 9) supports this claim with a significant increase in temperature between 650–750 m in depth. Burns and others (2015) identified a similar trend when developing a regional heat flow model for the Columbia basin and suggested that active groundwater circulation in shallower units could be transporting heat laterally away from its source and suppressing the geothermal gradient at shallower depths—implying that there is elevated heat flux masked by a strong regional groundwater flow regime. Following this thread, the deeper CRBG aquifer groundwaters are more mineralized because the elevated heat (1) reduces carbonate solubility leading to calcite oversaturation in some samples (Fig. 9) with precipitation of carbonate in the pore spaces, and (2) increases silicate mineral solubility with continued undersaturation of silica and basaltic glass (Fig. 11) and amplified rates of hydrolysis and cation exchange reactions. The much lower groundwater flow rates in the deeper CRBG aquifer lead to increased levels of mineralization.

The result is a stacked aquifer system of laterally extensive flow units with a persistent horizon that acts as a vertical barrier for groundwater chemistry, truncating actively circulating freshwater that overlies a deeper, relatively stagnant and mineralized groundwater. While these data show the change in chemistry to be at 650–750 m in depth, it is important to note that the paucity of deep samples from the basin periphery makes basin-wide extrapolation of the existence and depth of this change in chemistry difficult. The hydraulic reason of this feature is not entirely clear as it could be a zone of exceptionally high permeability that shunts groundwater laterally in the upper aquifer and prevents downward mixing or a low permeability layer that greatly reduces the vertical penetration of the overlying freshwater (Burns and others, 2015). Both types of laterally extensive contrasts in vertical permeability are present in the CRBG, and both are known to occur at the top of the Sentinel Bluffs Member, the youngest set of basalt flows of the Grande Ronde Basalt (Reidel and others, 2005).

For example, widespread and long-lasting subaerial exposure at the end of Sentinel Bluff times (~ 15 Ma) caused pervasive chemical weathering in the uppermost Grande Ronde Basalt, annealing fractures and filling vesicles with clays and other alteration products that reduce permeability. In another example, the widespread deposition of fluvial and lacustrine sediments by the proto-Columbia and Snake Rivers and their tributaries resulted in the Vantage Horizon of the Ellensburg Formation that separates the Grande Ronde Basalt from the Wanapum Basalt. In some regions, the Vantage Horizon is a sandstone with high permeability (Lindsey and others 2009). In other regions, the Vantage Horizon is clay rich and of low permeability (McGrail and others, 2009). In all cases, the overlying Eckler Mountain Member of the Wanapum Basalt includes extensive breccia, pillow-palagonite, and hyaloclastite facies at its base (Reidel and others, 2013), creating a zone of enhanced permeability.

Measured values of TDS in this dataset for the CRBG aquifer system are $<10,000$ mg/L, even at depths $>1,000$ m (Fig. 10). Although the ^{14}C data imply that CRBG groundwater >750 m is at least Pleistocene in age (Fig. 8), these deep groundwaters are not saline, unlike the TDS values in most sedimentary basins (Ferguson and others, 2018). There are several likely contributing factors. First, there has not been enough time for water-rock reactions to reach equilibrium—deep CRBG groundwater remains undersaturated with respect to basalt mineral phases (Fig. 13). Second, the CRBG basalt flows were emplaced in a deepening continental backarc basin—the connate groundwaters were meteoric and not marine in origin. Third, the CRBG are igneous in origin, and do not include significant organic matter, excepting the intercalated organics of interflow horizons. Because of this, the basin is largely free of the catagenesis that drives hydrocarbon production and associated thermogenic sulfate reduction that rapidly drives up TDS to produce brine (Machel, 2001). While there was oil and gas exploration in the Columbia basin, and data from some of those wells are included in this dataset, those exploration wells were largely penetrative of the CRBG into the sub-basalt sedimentary facies. Some of the data from oil and gas wells are not conclusive of actual conditions

at depth since it is possible that the chemistry is modified by the presence of drilling fluids.

The $\delta^{18}\text{O}$ and $\delta^2\text{H}$ data from this study provide some additional insight to groundwater age. There is an increased depletion of the heavier isotope from the surface to a depth of 650 m. Shallow groundwaters in the Wanapum and Saddle Mountain basalts have $\text{pmc} > 80\%$ and have $\delta^{18}\text{O}$ values that are consistent with mean modern precipitation (Robertson and Gazis, 2006)—they experience significant meteoric flushing. Groundwaters at a depth of 650–750 m have $\text{pmc} < 20\%$ with isotopic values consistent with recharge sourced to higher elevations and (or) colder climates—potentially the result of glacial meltwaters from repeated cycles of Pleistocene Missoula floods (Brown and others, 2010)—those groundwaters have been preserved because meteoric flushing does not penetrate the vertical permeability barrier. Below 750 m in the Grande Ronde Basalt, $\delta^{18}\text{O}$ data are absent, but $\delta^2\text{H}$ data trend toward less depletion, with some samples more enriched in the heavier isotope than modern precipitation. It is possible that some of these deep CRBG groundwaters were connate to basalt emplacement, when CO_2 emissions from the CRBG volcanism may have led to higher global temperatures, and thus enrichment in the heavier isotope, during the Mid-Miocene Climate Optimum (Kasbohm and Schoene, 2018).

Spatial distribution of CRBG groundwater types

Emplacement of the CRBG occurred over a wide geographic region that at its core includes the Columbia basin, but also includes portions of the Blue Mountains, the Yakima Fold and Thrust Belt, and the eastern margin of the Cascade Range. The suite of samples in this study comes from four of these physiographic provinces (Fig. 4), that are part of the Columbia basin. The previous section identified the persistence of vertical stratification in the CRBG aquifer system. There are also geographic differences along an east-west transect bisected by the Columbia River. The combined PCA and HCA from this study further express this geographic variation. Key analytes and isotopic measurements provide greater context to the reasons for these differences. We will discuss each in turn.

CRBG GROUNDWATER GROUPS

The Group 1 samples identified in the HCA are typical Ca-Mg- HCO_3 -type groundwater and span all CRBG formations. They are generally from < 650 m depth and originate from all geographies of CRBG exposure (Fig. 17). Oxidation and carbonation reactions between meteoric recharge and basalt occur at near-ambient temperatures.

Group 2 samples are mostly from > 750 m depth in the Grande Ronde Basalt and associated with the Yakima Fold and Thrust Belt (Fig. 17). Many samples from this group are from the Hanford Site and were part of detailed subsurface characterization

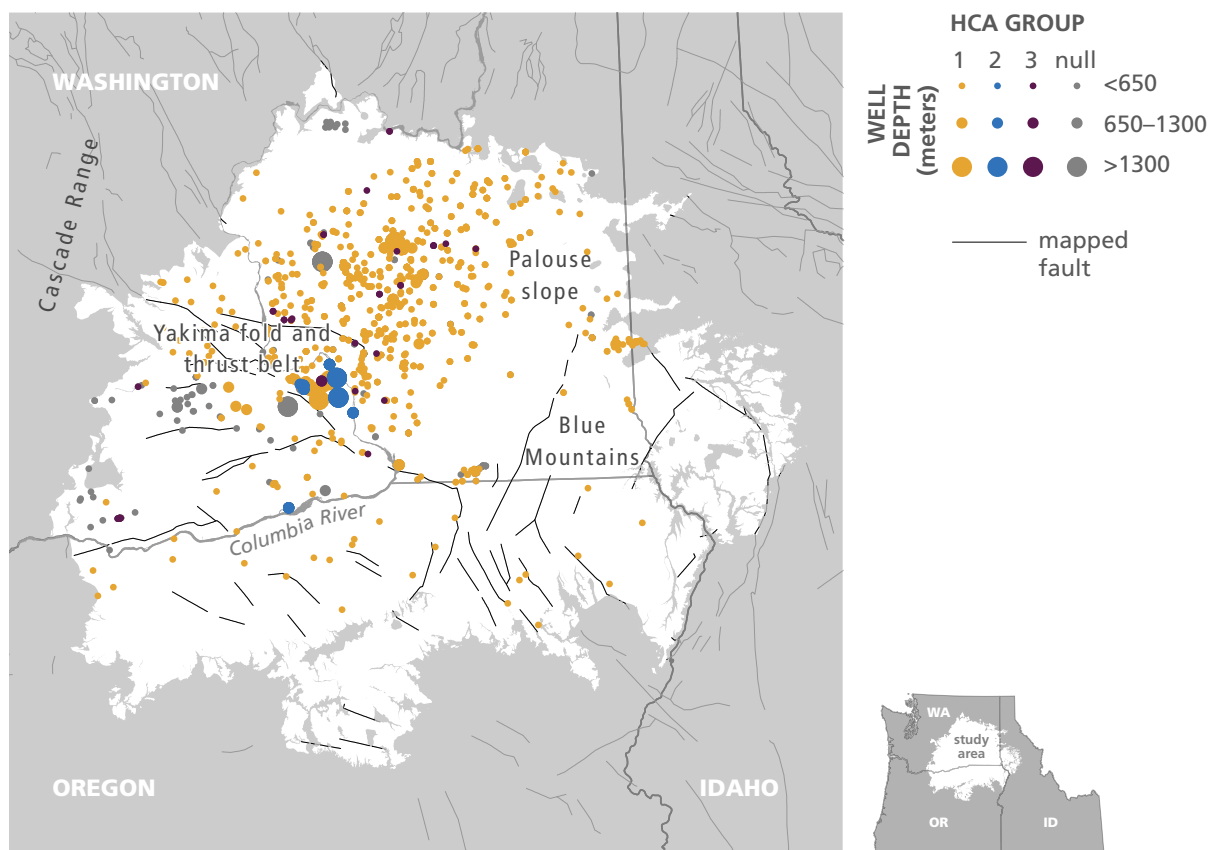


Figure 17. Map depicting the geographic boundary of a portion of the Columbia River Basalt Group in the Columbia Basin. The distribution of samples in the companion groundwater chemistry database are shown with sites classified by group from the hierarchical cluster analysis, while size is scaled according to well depth. Faults are shown as grey lines.

during the Basalt Waste Isolation Project (Carnahan, 1982). Hydrolysis and cation exchange reactions between the basalt and thermal fluids in alkaline and reducing conditions lead to Na-Cl-type groundwaters that are additionally enriched in $[F^-]$, $[Al]$, and $[SO_4^{2-}]$.

Riley and others (1990) noted that CRBG groundwater at the Hanford Site differs from groundwater elsewhere in the Columbia basin. This may be the product of specific geologic conditions at the Hanford site; elevated $[F^-]$ in some Hanford wells were sourced to an enrichment of fluoride-bearing minerals in portions of the Ellensburg Formation. However, the lack of deep samples for other portions of the Columbia basin limits this extrapolation. For example, the 100 Circles oil and gas well located south of Wallula Gap and along the Columbia River near the border with Oregon is completed in the deep Grande Ronde and is a part of the suite of Group 2 samples. What is common among all Group 2 samples is that they come from an area where the CRBG is thick and modified by regional folds and faults that may guide additional inputs from deeper, thermal groundwaters from the sub-basalt basement.

The Group 3 samples are a special case of samples from <650 m depth that have elevated TDS (Fig. 17). This group comprises two sub-groups. Many of the samples belonging to Group 3 are from the central, agricultural portion of the Columbia basin. While still categorized as Ca-Mg- HCO_3^- -type groundwater, these samples have elevated $[TN]$, $[Cl^-]$, and $[SO_4^{2-}]$ that reflect inputs of fertilizer. The remaining Group 3 samples are from soda springs and wells from CRBG exposures in the western margin that are highly elevated in $[HCO_3^-]$. The CO_2 at these sites likely derives from volcanic sources in the Cascades and migrates along structures of the Yakima Fold and Thrust Belt. (Mariner and others, 1982).

ISOTOPIC PROFILE OF CRBG GROUNDWATER

The isotopic profile of the samples provides some additional clarity. Values of $\delta^{18}O$ are slightly more depleted in the heavier isotope west of the Columbia River in Group 2 and in some Group 3 samples. This could be explained by source waters that originate from higher elevations along the margins of the Cascade Mountains. Water east of the Columbia River originates from the Columbia basin, or infiltrates at lower elevations along the CRBG margins in the Palouse Slope and Blue Mountains.

An important process that may affect $\delta^{18}O$ is the exchange of oxygen between thermal groundwater, basalt minerals (Cole and Ohmoto, 1986), and dissolved CO_2 (Karolyte and others, 2017). This ion exchange can deplete the heavier isotope since ^{18}O is more depleted both in igneous minerals and in CO_2 that originates from magmatic fluids or from organic decomposition. Since Group 2 samples are from deeper settings in the Yakima folds, it is possible that depletion of ^{18}O occurs along the steeply descending flow paths in and along the flanks of folds and faults.

The $\delta^{13}C$ of dissolved inorganic carbon and $\delta^{34}S$ in dissolved sulfate support the above interpretations and provide additional context. Samples in Groups 1 and the agricultural subset of Group 3, largely east of the Columbia River, have $\delta^{13}C$ values that reflect mixing between atmospheric CO_2 and the decomposed C4 vegetation that is prevalent in the semi-arid

Columbia basin. The $\delta^{34}S$ of Group 1 samples is progressively more enriched in ^{34}S with depth. This reflects sulfur sources in shallow groundwater that originate from atmospheric deposition and water-rock interactions with sulfide minerals in basalt, and interactions between deeper groundwater and Mesozoic sedimentary rocks of marine origin that underlie the CRBG in portions of the Palouse Slope.

The samples in Group 2 and the mineral spring subset of Group 3, west of the Columbia River, have $\delta^{13}C$ values that are both highly enriched and highly depleted (see figures in data supplement). Those with ^{13}C enrichment are likely from thermogenic CO_2 production, including inputs of magmatic CO_2 . Those with ^{13}C depletion are likely from biogenic CO_2 production from organic reduction and methanogenesis in the underlying Paleogene sediments and CRBG interflow horizons. The $\delta^{34}S$ of samples from this group follow this interpretation. They include some values that are consistent with atmospheric deposition of sulfate, sulfide minerals in basalt, and volcanogenic gas, and other values that may have some depletion of ^{34}S due to thermogenic sulfate reduction.

CONCLUSIONS

This study aggregates and synthesizes the largest-to-date collection of groundwater chemistry data associated with the Columbia River Basalt Group. The 1,537 samples in the accompanying dataset include sites from all areas of the Columbia basin and from all CRBG formations from the surface to depths >1,300 m. The results support the range of observations noted by more than a century of investigation and highlight regional variation by using robust comparative and statistical analyses on 26 analytes. These variations include both vertical and lateral anisotropy in groundwater chemistry. In addition to variations with depth in dissolved ions, stable isotopes, and radioactive carbon, this study also identifies patterns between these analytes and the geologic setting.

Evaluations of the groundwater chemistry database and modeled mineral solubility kinetics support the alteration of basalt to oxide and clay minerals with a concurrent release of alkaline-earth metals into solution at depths up to 650 m. This occurs because high-permeability flow horizons in the Wanapum and Saddle Mountains basalts convey meteoric recharge of neutral pH and oxidizing conditions to depths up to 650 m.

There is a persistent transition in water chemistry at depths from 650–750 m, with sample bias toward the center of the Columbia basin, that may represent a base of active groundwater circulation and Holocene meteoric flushing. This transition may be the result of a high-permeability zone at the base of the Wanapum Basalt or a low permeability zone at the top of the Grande Ronde Basalt, or both, that separates an upper and a lower CRBG aquifer. We present no complementary data from core descriptions to identify the source of permeability contrast, but reasons may include: interflow sediments of variable permeability; fracture annealing from subaerial exposure between flows; mineralization in porosity from changes to carbonate solubility, or active weathering by warmer waters at depth. This transition zone is marked by a rapid increase in temperature in

Pleistocene groundwaters that have lower $\delta^{18}\text{O}$ values and could be derived from the Missoula floods.

Groundwaters in the lower CRBG aquifer at depths >750 m are thermal, anoxic, alkaline, and comparatively stagnant. Alkaline-earth metals in these deeper groundwaters are mostly absent, lost to carbonate precipitation and cation exchange. Increased salinity in the lower CRBG aquifer is from greater alkali metal concentrations. Other dissolved ions prevalent in the lower CRBG aquifer, such as chlorine, fluorine, sulfate, and aluminum may be sourced from mineral weathering along deep flow paths in the Yakima Fold and Thrust Belt, from interactions with the sub-basalt geology as noted from the sulfur isotopes in deeper samples of the Palouse Slope, or from the incorporation of magmatic gas and fluids as noted by carbon isotopes in some soda-rich springs and wells in the eastern margin of the Cascade Volcanic Arc.

Perhaps most telling about the origin of CRBG groundwater is that only three of the samples in this compilation are saline. The highest concentrations of total dissolved solids are less than 1,700 mg/L except for three deep oil and gas wells, even at depths >1,300 m. While it is possible, and even quite likely, that CRBG groundwaters at depths more than 3,000 m are saline, the lack of samples at these depths prevents that extrapolation. The freshwater nature of most CRBG groundwater, even waters that may be coeval with the emplacement of basalt, is notable and speaks to the meteoric origins of the groundwater in the Columbia basin and the pace of water-rock interactions in these deeper settings. Given the regulatory requirements in place to protect potential sources of potable groundwater from the impacts of thermal energy storage and carbon sequestration projects, future studies will be needed to more fully characterize deep CRBG groundwater outside the scope of this published database.

ACKNOWLEDGMENTS

This study is the culmination of extensive work by colleagues and peers in the Columbia River Basalt Group and the Columbia Plateau Regional Aquifer System. We are particularly indebted to conversations with and commentary by Terry Tolan, Steve Reidel, and Erick Burns. Portions of the content herein stemmed from a one-day workshop on the “Big Questions” in the Columbia Basin hosted by the Washington Geological Survey and held at Central Washington University in Ellensburg, Washington. The companion database to this report includes references to the sources of data that were aggregated. We are especially thankful for the peer reviews provided by Tracy Branam of the Indiana Geological and Water Survey, Kelly Deuring of the University of Omaha, Stephani DiRaddo of the Pacific Northwest National Laboratories, and Robert Perkins of Portland State University. Joel Gombiner of the WGS Publications Group did enormous work preparing the figures and managing the review.

REFERENCES

- Aradóttir, E. S. P.; Sonnenthal, E. L.; Jónsson, H., 2012, Development and evaluation of a thermodynamic dataset for phases of interest in CO_2 mineral sequestration in basaltic rocks: *Chemical Geology*, v. 304–305, p. 26–38. [https://doi.org/10.1016/j.chemgeo.2012.01.031]
- Baker, L. L.; Rember, W. C.; Sprenke, K. F.; Strawn, D. G., 2012, Celadonite in continental flood basalts of the Columbia River Basalt Group: *American Mineralogist*, v. 97, no. 8–9, p. 1284–1290. [https://doi.org/10.2138/am.2012.4129]
- Baker, L. L.; Neill, O. K., 2017, Geochemistry and mineralogy of a saprolite developed on Columbia River Basalt: Secondary clay formation, element leaching, and mass balance during weathering: *American Mineralogist*, v. 102, no. 8, p. 1632–1645. [https://doi.org/10.2138/am-2017-5964]
- Barry, T. L.; Self, S.; Kelley, S. P.; Reidel, S.; Hooper, P.; Widdowson, M., 2010, New $^{40}\text{Ar}/^{39}\text{Ar}$ dating of the Grande Ronde lavas, Columbia River Basalts, USA: Implications for duration of flood basalt eruption episodes: *Lithos*, v. 118, no. 3–4, p. 213–222. [https://doi.org/10.1016/j.lithos.2010.03.014]
- Bauer, H. H.; Hansen, A. J., 2000, Hydrology of the Columbia Plateau regional aquifer system, Washington, Oregon, and Idaho: U.S. Geological Survey Water-Resources Investigations Report 96-4106. [https://doi.org/10.3133/wri964106]
- Benson, L. V.; Teague, L. S., 1982, Diagenesis of basalts from the Pasco Basin, Washington; I. Distribution and composition of secondary mineral phases: *Journal of Sedimentary Research*, v. 52, no. 2, p. 595–613. [https://doi.org/10.1306/212F7FAE-2B24-11D7-8648000102C1865D]
- Bethke, C. M., 2008, Geochemical and biogeochemical reaction modeling: Cambridge University Press, 543 p. [https://doi.org/10.1017/CBO9780511619670]
- Brown, K. B.; McIntosh, J. C.; Baker, V. R.; Gosch, Damian, 2010, Isotopically-depleted late Pleistocene groundwater in Columbia River Basalt aquifers: Evidence for recharge of glacial Lake Missoula floodwaters?: *Geophysical Research Letters*, v. 37, no. 21. [https://doi.org/10.1029/2010GL044992]
- Burns, E. R.; Williams, C. F.; Ingebritsen, S. E.; Voss, C. I.; Spane, F. A.; DeAngelo, J., 2015, Understanding heat and groundwater flow through continental flood basalt provinces: insights gained from alternative models of permeability/depth relationships for the Columbia Plateau, USA: *Geofluids*, v. 15, p. 120–138. [https://doi.org/10.1111/gfl.12095]
- Burns, E. R.; Bershaw, John; Williams, C. F.; Wells, Ray; Uddenberg, Matt; Scanlon, Darby; Cladouhos, Trenton; Van Houten, Boz, 2020, Using saline or brackish aquifers as reservoirs for thermal energy storage, with example calculations for direct-use heating in the Portland Basin, Oregon, USA: *Geothermics*, v. 88, article 101877. [https://doi.org/10.1016/j.geothermics.2020.101877]
- Burt, Walter; Conlon, Terrence; Tolan, T. L.; Wells, R. E.; Melady, Jason, 2009, Hydrogeology of the Columbia River Basalt Group in the northern Willamette Valley, Oregon. In O'Connor, J. E.; Dorsey, R. J.; Madin, I. P., *Volcanoes to Vineyards: Geologic field trips through the dynamic landscape of the Pacific Northwest: The Geological Society of America Field Guide* 15, p. 697–736. [https://doi.org/10.1130/2009.fld015(31)]
- Cao, Ruoshi; Miller, Q. R. S.; Davidson, C. L.; Gallin, William; Reidel, S. P.; Jiao, Zunsheng; McLaughlin, Fred; Nienhuis, E. T.; Schaefer, H. T., 2024, Gigaton commercial-scale carbon storage and mineralization potential in stacked Columbia River basalt reservoirs: *International Journal of Greenhouse Gas Control*, v. 137, article 104206. [https://doi.org/10.1016/j.ijggc.2024.104206]
- Carnahan, C. L., 1982, Selected hydrologic and geochemical issues in site characterization for nuclear waste disposal: Flood basalts at the Hanford Reservation: Lawrence Berkeley Laboratory, 165 p.
- Cole, D. R.; Ohmoto, H., 1986, Kinetics of isotopic exchange at elevated temperatures. In Valley, J. W.; Taylor, H. P.; O'Neil, J. R. Jr., editors, *Stable isotopes in high temperature geological processes: Reviews in Mineralogy & Geochemistry*, v. 16. [https://doi.org/10.1515/9781501508936]

- Craig, Harmon, 1961, Isotopic variations in meteoric waters: *Science*, v. 133, p. 1702–1703. [https://doi.org/10.1126/science.133.3465.1702]
- Cummings, M. L.; Trone, P. M.; Pollock, J. M., 1989, Geochemistry of colloidal silica precipitates in altered Grande Ronde Basalt, northeastern Oregon, USA: *Chemical Geology*, v. 75, no. 1–2, p. 61–79. [https://doi.org/10.1016/0009-2541(89)90021-1]
- Deutsch, W. J.; Jenne, E. A.; Krupka, K. M., 1982, Solubility equilibria in basalt aquifers: the Columbia Plateau, eastern Washington, USA: *Chemical Geology*, v. 36, no. 1–2, p. 15–34. [https://doi.org/10.1016/0009-2541(82)90037-7]
- Duckett, K. A.; Langman, J. B.; Bush, J. H.; Brooks, E. S.; Dunlap, Pamela; Stanley, J. R., 2020, Noble gases, dead carbon, and reinterpretation of groundwater ages and travel time in local aquifers of the Columbia River Basalt Group: *Journal of Hydrology*, v. 581, article 124400. [https://doi.org/10.1016/j.jhydrol.2019.124400]
- Environmental Protection Agency (EPA), 2024, Secondary Drinking Water Standards: Guidance for Nuisance Chemicals. [accessed April 23, 2025 at https://www.epa.gov/sdwa/secondary-drinking-water-standards-guidance-nuisance-chemicals].
- Farquhar, G. D.; Ehleringer, J. R.; Hubick, K. T., 1989, Carbon isotope discrimination and photosynthesis: *Annual Review of Plant Biology*, v. 40, p. 503–537. [https://doi.org/10.1146/annurev.pp.40.060189.002443]
- Faure, Gunter, 1986, Principles of isotope geology, second edition: John Wiley & Sons, 589 p.
- Ferguson, Grant; McIntosh, J. C.; Grasby, S. E.; Hendry, M. J.; Jasechko, Scott; Lindsay, M. B.; Luijendijk, Elco, 2018, The persistence of brines in sedimentary basins: *Geophysical Research Letters*, v. 45, no. 10, p. 4851–4858. [https://doi.org/10.1029/2018GL078409]
- Ferguson, H. F., 1967, Valley stress release in the Allegheny Plateau: *Engineering Geology*, v. 4, no. 1, p. 63–71.
- Forson, Corina; Swyer, M. W.; Schmalzle, G. M.; Czajkowski, J. L.; Cladouhos, T. T.; Davatzes, Nichloas; Norman, D. K.; Cole, R. A., 2015, Geothermal play-fairway analysis of Washington State prospects: *Transactions - Geothermal Resources Council*, v. 39. [https://www.osti.gov/biblio/1839964]
- Hansen, A. J., Jr.; Vaccaro, J. J.; Bauer, H. H., 1994, Ground-water flow simulation of the Columbia Plateau regional aquifer system, Washington, Oregon, and Idaho: U.S. Geological Survey Water-Resources Investigations Report 91-4187, 81 p., 15 plates. [https://doi.org/10.3133/wri914187]
- Hearn, P. P., Jr.; Steinkampf, W. C.; Horton, D. G.; Solomon, G. C.; White, L. D.; Evans, J. R., 1989, Oxygen-isotope composition of ground water and secondary minerals in Columbia Plateau basalts: implications for the paleohydrology of the Pasco Basin: *Geology*, v. 17, no. 7, p. 606–610. [https://doi.org/10.1130/0091-7613(1989)017<0606:OICOGW>2.3.CO;2]
- Hearn, P. P., Jr.; Steinkampf, W. C.; White, L. D.; Evans, J. R., 1990, Geochemistry of rock-water reactions in basalt aquifers of the Columbia River Plateau. *In* Proceedings of a U.S. Geological Survey workshop on environmental geochemistry: U.S. Geological Survey Circular 1033. [https://doi.org/10.3133/cir1033]
- Hooper, P. R., 1982, The Columbia River basalts: *Science*, v. 215, no. 4539, 1463–1468. [https://doi.org/10.1126/science.215.4539.1463]
- Hooper, P. R.; Conrey, R. M., 1989, A model for the tectonic setting of the Columbia River basalt eruptions. *In* Reidel, S. P.; Hooper, P. R., editors, Volcanism and tectonism in the Columbia River flood-basalt province: Geological Society of America Special Papers v. 239. [https://doi.org/10.1130/SPE239-p293]
- Johnson, H. M.; Ely, Kate; Maher, A. T., 2024, Timing and source of recharge to the Columbia River Basalt groundwater system in northeastern Oregon: *Groundwater*, v. 62, no. 5, p. 761–777. [https://doi.org/10.1111/gwat.13404]
- Johnson, J.; Anderson, G.; Parkhurst, D., 2000, Database “thermo.com. V8. R6. 230,” Rev. 1-11: Lawrence Livermore National Laboratory.
- Kahle, S. C.; Morgan, D. S.; Welch, W. B.; Ely, D. M.; Hinkle, S. R.; Vaccaro, J. J.; Orzol, L. L., 2011, Hydrogeologic framework and hydrologic budget components of the Columbia Plateau regional aquifer system, Washington, Oregon, and Idaho: U.S. Geological Survey Scientific Investigations Report 2011-5124. [https://doi.org/10.3133/sir20115124]
- Karolytė, Rūta; Serno, Sascha; Johnson, Gareth; Gilfillan, S. M. V., 2017, The influence of oxygen isotope exchange between CO₂ and H₂O in natural CO₂-rich spring waters: Implications for geothermometry: *Applied Geochemistry*, v. 84, p. 173–186. [https://doi.org/10.1016/j.apgeochem.2017.06.012]
- Kasbohm, Jennifer; Schoene, Blair, 2018, Rapid eruption of the Columbia River flood basalt and correlation with the mid-Miocene climate optimum: *Science Advances*, v. 4, no. 9. [https://doi.org/10.1126/sciadv.aat8223]
- Kolawole, Folarin; Evenick, J. C., 2023, Global distribution of geothermal gradients in sedimentary basins: *Geoscience Frontiers*, v. 14, no. 6, article 101685. [https://doi.org/10.1016/j.gsf.2023.101685]
- Larson, K. R.; Keller, C. K.; Larson, P. B.; Allen-King, R. M., 2005, Water resources implications of ¹⁸O and ²H distributions in a basalt aquifer system: *Groundwater*, v. 38, no. 6, p. 947–953. [https://doi.org/10.1111/j.1745-6584.2000.tb00695.x]
- Lindsey, Kevin; Morgan, David; Vlassopoulos, Dimitri; Tolan, T. L.; Burns, Eric, 2009, Hydrogeology of the Columbia River Basalt Group in the Columbia Plateau: Road log and field trip stop descriptions. *In* O’Connor, J. E.; Dorsey, R. J.; Madin, I. P., editors, Volcanoes to vineyards, Geologic field trip through the dynamic landscape of the Pacific Northwest: Geological Society of America Field Trip Guide, v. 15. [https://doi.org/10.1130/2009.fld015(30)]
- Lite, K. E., 2013, The influence of depositional environment and landscape evolution on groundwater flow in Columbia River Basalt—Examples from Mosier, Oregon. *In* Reidel, S. P.; Camp, V. E.; Ross, M. E.; Wolff, J. A.; Martin, B. S.; Tolan, T. L.; Wells, R. E., editors, The Columbia River flood basalt province: Geological Society of America Special Paper 497. [https://doi.org/10.1130/2013.2497(17)]
- Long, P. E.; Wood, B. J., 1986, Structures, textures, and cooling histories of Columbia River basalt flows: *Geological Society of America Bulletin*, v. 97 no. 9, p. 1144–1155. [https://doi.org/10.1130/0016-7606(1986)97<1144:STACHO>2.0.CO;2]
- Machel, H. G., 2001, Bacterial and thermochemical sulfate reduction in diagenetic settings—old and new insights: *Sedimentary Geology*, v. 140, no. 1–2, p. 143–175. [https://doi.org/10.1016/S0037-0738(00)00176-7]
- Mariner, R. H.; Presser, T. S.; Evans, W. C., 1982, Chemical and isotopic composition of water from thermal and mineral springs of Washington: U.S. Geological Survey Open-File Report 82-98, 18 p. [https://pubs.usgs.gov/of/1982/0098/report.pdf]
- McGrail, B. P.; Sullivan, E. C.; Spane, F. A.; Bacon, D. H.; Hund, G.; Thorne, P. D.; Thompson, C. J.; Reidel, S. P.; Colwell, F. S., 2009, Preliminary hydrogeologic characterization results from the Wallula Basalt Pilot Study: Battelle Pacific Northwest Division PNWD-4129. [https://www.researchgate.net/publication/236496904_Preliminary_Hydrogeologic_Characterization_Results_from_the_Wallula_Basalt_Pilot_Study]
- Medici, Giacomo; Langman, J. B., 2022, Pathways and estimate of aquifer recharge in a flood basalt terrain: A review from the South Fork Palouse River basin (Columbia River Plateau, USA): *Sustainability*, v. 14, no. 18, p. 11349. [https://doi.org/10.3390/su141811349]

- Nelson, Dennis; Melady, Jason, 2014, Denitrification in a deep basalt aquifer: implications for aquifer storage and recovery: *Groundwater*, v. 52, no. 3, p. 414–423. [<https://doi.org/10.1111/gwat.12082>]
- Paytan, Adina; Kastner, Miriam; Campbell, Douglas; Thiemens, M. H., 1998, Sulfur isotopic composition of Cenozoic seawater sulfate: *Science*, v. 282, p. 1459–1462 [<https://doi.org/10.1126/science.282.5393.1459>]
- Reidel, S. P.; Spane, F. A.; Johnson, V. G., 2005, Potential for natural gas storage in deep basalt formations at Canoe Ridge, Washington State: a hydrogeologic assessment: Pacific Northwest National Lab PNNL-15386. [https://www.pnnl.gov/main/publications/external/technical_reports/PNNL-15386.pdf]
- Reidel, S. P.; Camp, V. E.; Tolan, T. L.; Martin, B. S., 2013, The Columbia River flood basalt province: stratigraphy, areal extent, volume, and physical volcanology. *In* Reidel, S. P.; Camp, V. E.; Ross, M. E.; Wolff, J. A.; Martin, B. S.; Tolan, T. L.; Wells, R. E., editors, *The Columbia River flood basalt province: Geological Society of America Special Paper 497*. [[https://doi.org/10.1130/2013.2497\(01\)](https://doi.org/10.1130/2013.2497(01))]
- Reidel, S. P.; Camp, V. E.; Martin, B. S.; Tolan, T. L.; Wolff, J. A., 2016, The Columbia River Basalt Group of western Idaho and eastern Washington—Dikes, vents, flows, and tectonics along the eastern margin of the flood basalt province. *In* Lewis, R. S.; Schmidt, K. L., editors, *Exploring the geology of the inland Northwest: Geological Society of America Field Guide 41*. [[https://doi.org/10.1130/2016.0041\(04\)](https://doi.org/10.1130/2016.0041(04))]
- Riley, J. A.; Steinhurst, R. K.; Winter, G. V.; Williams, R. E., 1990, Statistical analysis of the hydrochemistry of ground waters in Columbia River basalts: *Journal of Hydrology*, v. 119, no. 1–4, p. 245–262. [[https://doi.org/10.1016/0022-1694\(90\)90045-Y](https://doi.org/10.1016/0022-1694(90)90045-Y)]
- Robertson, J. A.; Gazis, C. A., 2006, An oxygen isotope study of seasonal trends in soil water fluxes at two sites along a climate gradient in Washington State (USA): *Journal of Hydrology*, v. 328, no. 1–2, p. 375–387. [<https://doi.org/10.1016/j.jhydrol.2005.12.031>]
- Soderberg, E. R.; Wolff, J. A., 2023, Mantle source lithologies for the Columbia River flood basalt province: *Contributions to Mineralogy and Petrology*, v. 178, no. 2, article 11. [<https://doi.org/10.1007/s00410-023-01993-2>]
- Steinkampf, W. C.; Hearn, P. P., Jr., 1996, Ground-water geochemistry of the Columbia Plateau aquifer system, Washington, Oregon, and Idaho: US Geological Survey Open-File Report 95-467. [<https://doi.org/10.3133/ofr95467>]
- Steinkampf, W.C.; Bortleson, G.C.; Packard, F.A., 1985, Controls on ground-water chemistry in the Horse Heaven Hills, south-central Washington: U.S. Geological Survey Water-Resources Investigations Report 85-4048, 26 p. [<https://doi.org/10.3133/wri854048>]
- Svadenak, E. E., 2019, Geochemical response to thermal energy storage in the Columbia River Basalt Aquifer System beneath the Portland Basin, Oregon: Portland State University Master of Science thesis, 116 p. [https://pdxscholar.library.pdx.edu/open_access_etds/5362/]
- Tipple, B. J.; Meyers, S. R.; Pagani, Mark, 2010, Carbon isotope ratio of Cenozoic CO₂: A comparative evaluation of available geochemical proxies: *Paleoceanography*, v. 25, no. 3, article PA3202. [<https://doi.org/10.1029/2009PA001851>]
- Tolan, T. L.; Martin, B. S.; Reidel, S. P.; Anderson, J. L.; Lindsey, K. A.; Burt, W., 2009a, An introduction to the stratigraphy, structural geology, and hydrology of the Columbia River flood basalt province: A primer for the GSA Columbia River Basalt Group field trips. *In* O'Connor, J. E.; Dorsey, R. J.; Madin, I. P., editors, *Volcanoes to vineyards: Geologic field trips through the dynamic landscape of the Pacific Northwest: Geological Society of America Field Trip Guide v. 15*. [[https://doi.org/10.1130/2009.fld015\(28\)](https://doi.org/10.1130/2009.fld015(28))]
- Tolan, T. L.; Martin, B. S.; Reidel, S. P.; Kauffman, J. D.; Garwood, D. L.; Anderson, J. L., 2009b, Stratigraphy and tectonics of the central and eastern portions of the Columbia River flood-basalt province: An overview of our current state of knowledge. *In* O'Connor, J. E.; Dorsey, R. J.; Madin, I. P., editors, *Volcanoes to vineyards: Geologic field trips through the dynamic landscape of the Pacific Northwest: Geological Society of America Field Trip Guide v. 15*, p. 645–672. [[https://doi.org/10.1130/2009.fld015\(29\)](https://doi.org/10.1130/2009.fld015(29))]
- Tolan, T. L.; Lindsey, Kevin; Porcello, John, 2009c, A summary of Columbia River Basalt Group physical geology and its influence on the hydrogeology of the Columbia River Basalt Aquifer System: Columbia Basin Ground Water Management Area of Adams, Franklin, Grant, and Lincoln Counties.
- University of Cincinnati, 2018, UC Business Analytics R Programming Guide, Hierarchical Cluster Analysis: University of Cincinnati. [https://uc-r.github.io/hc_clustering]
- Vlassopoulos, Dimitri; Goin, Jessica; Zelif, Morgan; Porcello, John; Tolan, Terry; Lindsey, Kevin, 2009, Groundwater geochemistry of the Columbia River basalt group aquifer system—Columbia Basin groundwater management area of Adams, Franklin, Grant, and Lincoln Counties. Othello, Washington: The Columbia basin ground water management area of Adams, Franklin, Grant, and Lincoln Counties. [<https://apps.ecology.wa.gov/publications/documents/0912016.pdf>]
- Zakharova, N. V.; Goldberg, D. S.; Sullivan, E. C.; Herron, M. M.; Grau, J. A., 2012, Petrophysical and geochemical properties of Columbia River flood basalt: Implications for carbon sequestration: *Geochemistry, Geophysics, Geosystems*, v. 13, no. 11. [<https://doi.org/10.1029/2012GC004305>]

